Technical report; TR-194

KNMI

KNMI contribution to the European project POPSICLE

Theo Brandsma and T. Adri Buishand

De Bilt, 1996

Technical report = technisch rapport; TR-194

De Bilt, 1996

Postbus 201
3730 AE De Bilt
The Netherlands

Telephone +31.30.220 69 11, telefax +31.30.221 04 07

Authors: Theo Brandsma and T. Adri Buishand

UDC: 551.577.2
551.577.3
551.583.1
(4)
ISSN: 0169-1708
ISBN: 90-369-2114-7

● ● ● ●

KNMI contribution to the European project POPSICLE

Theo Brandsma and T. Adri Buishand

Royal Netherlands Meteorological Institute (KNMI), the Netherlands

Technical Report TR-194

Preface

This Technical Report presents the results of the KNMI-contribution to the European project POPSICLE (Production Of Precipitation Scenarios for Impact assessment of CLimate change in Europe). POPSCILE ran from 1 July 1994 until 30 September 1996. It was financed by the Commission of the European Union and the Swiss Foundation for Scientific Research.

The objective of POPSICLE was to develop and test new methods of producing climate change precipitation scenarios and to demonstrate their application to a range of sensitive European hydrological systems. Four river basins were chosen:

1. Tyne in northern England (2000 km^2),
2. Cobres in southern Portugal (700 km^2),
3. Arno in Italy (4000 km^2),
4. Broye in western Switzerland (400 km^2).

Six institutions participated in the project:

1. Project co-ordinator: University of Newcastle upon Tyne, Water Resource Systems Research Laboratory (Prof. P.E. O'Connell, C.G. Kilsby, Dr. P.S.P. Cowpertwait, C.S. Fallows);
2. KNMI (Dr T.A. Buishand, Dr T. Brandsma);
3. University of East Anglia, Climatic Research Unit (Dr. P.D. Jones, Dr. D. Conway);
4. Politecnico di Milano, Centro Interdipartimentale per le Ricerca in Informatica Territoriale e Ambientale (Prof. R. Rosso, Dr. P. Burlando);
5. Universidade de Lisboa, Instituto de Ciência Aplicade e Tecnologia (Prof. J. Corte-Real, Dr. E.Costa);
6. Ecole Polytechnique Fédérale de Lausanne, Institut d'Aménagement des Terres et des Eaux (Prof. A. Musy, Dr. D. Consuegra, A-C. Favre).

The present report describes the two research activities of KNMI in the POPSICLE project. In part I the precipitation-temperature dependence is described and its use for scenario production is discussed. Pat II deals with the comparison of atmospheric classification schemes.

Table of contents

Summary

Precipitation temperature dependence

Temperature determines the maximum moisture content of the air. The strength of convection is also controlled by temperature. Because of these factors, there is a link between precipitation and near-surface temperature. Advanced regression techniques were developed to describe the effect of temperature on the wet-day precipitation amounts. Three regions in Switzerland, England and Italy were considered. Airflow indices (vorticity, flow strength and direction) were used to account for the effect of the atmospheric circulation on precipitation. These airflow indices were the basic elements in an objective classification of the Lamb weather types as developed by Jenkinson and Collison in the 1970s. For the data in England and Italy the sea surface temperature turned out to be another important factor influencing the amount of precipitation.

For Switzerland, data from Bern, Neuchâtel and Payerne were analysed. For these stations the direction and strength of the flow are important airflow indices because of their influence on orographic precipitation enhancement. The data were divided in three categories of flow direction: (1) N/NE; (2) E/SE/S; and (3) SW/W/NW. For all three direction categories the mean wet-day precipitation amount generally increases with increasing temperature. The effect of the strength of the flow on the wet-day precipitation amounts varies with the flow direction. There is a strong positive relationship between the two variables for the SW-NW category. For the N/NE category precipitation tends to decrease with increasing strength of the flow. The effect of the strength of the flow could be neglected for the E-S category. Natural cubic splines and piecewise linear functions were used to describe non-linear effects of temperature and strength of the flow on the wet-day precipitation amounts.

For the English station Durham, the difference δ between the land and upstream sea surface temperature is an important predictor variable to unmask a positive temperature effect on precipitation. A relatively warm sea in the winter season enhances precipitation whereas the opposite occurs when the sea is relatively cold. Vorticity is the most important airflow index for Durham. There is, however, also a significant effect of the strength of the flow. To account for the dependence on flow direction, separate relationships were fitted for three categories of flow direction: (1) NE/E/SE; (2) S; and (3) SW/W/NW/N. The first category (rain coming from the adjacent North Sea) shows the strongest effect of δ and is further characterised by a positive dependence between the amount of precipitation and the strength of the flow. For the other two direction categories (rain coming from the land) there is a negative relationship between the wet-day precipitation amount and the strength of the flow. Vorticity has always a positive effect on the amount of precipitation, i.e. relatively much precipitation in cyclonic situations. All three direction categories show an almost exponential increase of the mean wet-day precipitation amount with increasing temperature.

For Italy, data from Florence and Livorno in Italy were considered. Despite the vicinity of the Apennines, the direction and strength of the flow have little influence on the wet-day precipitation amounts at these sites. The regression of precipitation on temperature, δ and vorticity was examined. The inclusion of δ strongly influences the estimated temperature effect. For Florence we also analysed the mean hourly amounts on wet days. These precipitation data show a stronger increase with increasing temperature than the mean wet-day amounts. This is due to the decrease of the mean wet-day rainfall duration with increasing temperature.

Empirical relationships between daily precipitation and temperature anomalies were studied. The anomalies were obtained by removing the annual cycles in the mean. Nevertheless, there still remained a clear seasonal variation in the relationships between the anomalies. On the other hand, the seasonal variation of the predictor variables quite well explained the annual cycle of the observed monthly mean precipitation amounts. For the Italian stations the inclusion of δ was necessary to reproduce the observed maximum mean rainfall for the autumn season.

Precipitation scenarios were derived for the case that there is a systematic increase in the air and sea surface temperatures and that there is no change in the airflow indices. According to the fitted relationships to the wet-day precipitation amounts, a warming of 3°C leads to an increase in mean annual precipitation of 7% (Neuchâtel) to 17% (Florence). The estimated increases are sensitive to the chosen predictor variables and the description of the temperature dependence in the regression models. An improvement of the physical basis of these models is needed to narrow the uncertainties of the estimated changes in precipitation.

Comparison of classification schemes for the Netherlands

The prediction of daily and monthly values of temperature, point precipitation and area-average precipitation was studied using the long-term daily averages of these elements for distinct weather types in the Netherlands. Three classification schemes have been compared: (1) the objective Lamb scheme; (2) The German Grosswetterlagen (GWL); and (3) an the objective P-27 scheme developed at KNMI.

For precipitation the three classification schemes perform almost equally well. They explain only 15 to 30% of the variance of daily precipitation characteristics and 40 to 60% of the variance of monthly rainfall. For the prediction of monthly area-average precipitation over the Netherlands the monthly average of the vorticity index in the objective Lamb scheme does at least as well as the daily class averages in the full classification scheme. The significant influence of vorticity has also been observed for precipitation in the UK.

For the 1949-1993 period the GWL and the P27 classification explain about 40% of the variance of the daily temperature and about 60% of the variance of the monthly temperature. The corresponding figures for the objective Lamb scheme are 29 and 42%, respectively. GWL performs less well for temperatures prior to 1949 when upper-air data were not available to define the weather types. A decrease in predictive skill for temperature data prior to 1949 is not found for the objective Lamb scheme.

PART I

Precipitation temperature dependence

1. Introduction

There is a link between the amount of precipitation and temperature. An important factor is the increase of the saturated vapour pressure with increasing temperature. Warm air can therefore contain more moisture than cold air. Mainly because of this temperature effect on atmospheric moisture, General Circulation Models (GCMs) predict that the global warming resulting from the increased atmospheric greenhouse gas concentrations will be accompanied by an increase in the global mean precipitation of 1.5–3% per °C temperature rise (IPCC, 1990,1992; Boer, 1993; Hulme, 1994). Besides the effect on the atmospheric water content, temperature also controls the strength of convection.

The dependence between precipitation and temperature is a somewhat neglected topic in the literature on climate change scenarios. Klein Tank and Buishand (1993) examined the relationship between the mean wet-day precipitation amount and temperature at De Bilt, an inland station in the Netherlands. The relationship was used to obtain scenarios of daily precipitation for a doubled CO_2 climate. The applicability of their approach to coastal sites and areas outside the Netherlands is questionable. An important condition is that a clear effect of temperature on precipitation must be identified for the site of interest.

Figure 1 shows the mean wet-day precipitation amount as a function of daily temperature for Durham (England), Bern (Switzerland), Beja (Portugal) and Florence (Italy). A day is considered to be wet if the amount of precipitation ≥ 0.3 mm. The diagrams for Bern and Beja show a considerable change in the mean wet-day precipitation amounts with increasing temperature but their shapes are quite different. On the other hand, there is little change in the mean wet-day precipitation amount for Durham and Florence. Obviously, a potential temperature effect is obscured by other meteorological factors at these sites. For Durham and Florence, the sea surface temperature has a significant effect on the form of the relationship in Fig. 1. Another important factor is the atmospheric flow. These factors have to be included in statistical models that describe the effect of temperature on precipitation.

Some factors influencing the amount of precipitation exhibit a clear annual cycle. Their influence on the wet-day precipitation amounts may also depend on the time of the year. Different options are available to account for seasonal variation. The incorporation of seasonal variation may, however, lead to an undesirable model complexity.

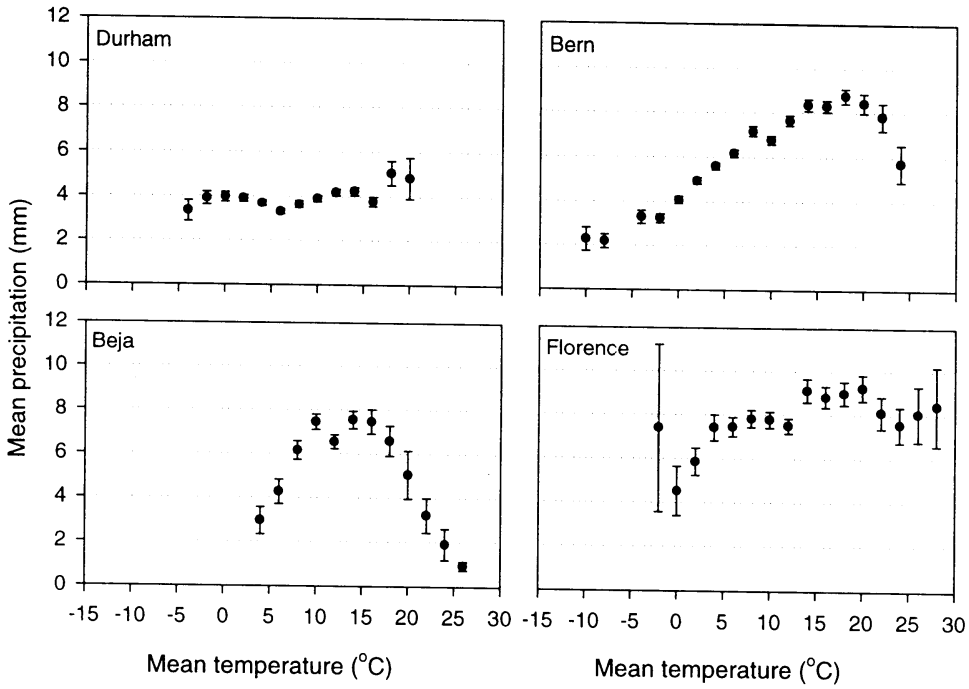

Figure 1: Relationship between daily mean precipitation and daily mean temperature for wet days (≥ 0.3 mm) at Durham (1931–1990), Bern (1901–1993), Beja (1957–1986) and Florence (1935–1987). The error bars give the standard error of the mean precipitation within each class. The total numbers of wet days for the four stations are 10128, 14062, 2584 and 4529, respectively.

In this part of the report the dependence of the wet-day precipitation amounts on temperature is analysed for Bern, Neuchâtel and Payerne in Switzerland[1], Durham in England, and Florence and Livorno in Italy. In section 2 we give an outline of the statistical methods used for linking precipitation to the predictor variables. Section 3 presents a detailed account of the inclusion of flow characteristics and sea surface temperatures. The need to incorporate seasonal variation is addressed in section 4. In section 5 we discuss the application to precipitation scenario production. Section 6 contains the conclusions.

2. Fitting models to observed relationships

In this section we present some background on statistical modelling of wet-day precipitation amounts. For ease of exposition we concentrate on the case of a single predictor variable (temperature T). The extension to more predictor variables is briefly discussed at the end of this section.

The wet-day precipitation amounts P have a highly skewed distribution. Days with small amounts predominate. Further, the standard deviation of P depends on the predictor variable(s). An interesting point is that the change in the coefficient of variation CV for different values of the predictor variable(s) is generally much smaller than that in the standard deviation. In quite a number of cases CV can be taken to be constant.

[1] A more detailed treatment of the Swiss data is accepted for publication in *Journal of Hydrology*.

Data with a constant *CV* can be modelled in two different ways (McCullagh and Nelder, 1989). The most widespread method is to define a linear model for the logarithm of *P*. The model can be fitted by ordinary least squares. For the wet-day precipitation amounts, this approach meets, however, two difficulties. First, the logarithm is sensitive to roundings of small precipitation amounts, and second, the assumption of a constant *CV* turns out to be rather crucial for the estimation of the mean of *P* from the fitted model (Klein Tank and Buishand, 1993). The alternative is to describe the untransformed wet-day precipitation amounts by a generalized linear model. Parameter estimation requires an Iteratively Reweighted Least Squares (IRLS) technique. The method can easily be extended to cases where *CV* is not constant. The second approach was therefore preferred in this study.

The amount of precipitation on a wet day with temperature T is represented as

$$P = \exp[g(T)] + \varepsilon \tag{1}$$

where $g(T)$ is a function of T and ε is a random error with zero mean. The first term on the right-hand side gives the expected value μ of P:

$$\mu = \mathrm{E}(P) = \exp[g(T)] \tag{2}$$

The change of the mean precipitation amount with T is thus determined by the function $g(T)$. For the linear model:

$$g(T) = a + bT \tag{3}$$

the mean increases exponentially with increasing T. In a number of cases quadratic and cubic terms in T were needed to describe the temperature effect on P. An essential condition for the IRLS technique is that $g(T)$ is linear in unknown regression coefficients like a and b.

Because of the exponential function in Eq.(1) the mean μ cannot be negative. The error ε is bounded by $-\mu$ because P must be positive. A more important aspect for parameter estimation is that the variance of ε depends on μ as well. For the case of a constant coefficient of variation var $\varepsilon = c^2\mu^2$, where c is a constant.

To reduce computer time, the model is fitted to the mean wet-day precipitation amounts in the various temperature classes instead of to the individual observations (Buishand and Klein Tank, 1996). This also provides a goodness of fit test. Assume that the domain of the explanatory variables can be partitioned into K different classes, then the adequacy of the fit can be tested with the deviance statistic:

$$D = 2\sum_{k=1}^{K} n_k \left[\frac{\overline{P}_k - \hat{\mu}_k}{\hat{\mu}_k} - \ln(\overline{P}_k / \hat{\mu}_k) \right] \Big/ CV_k^2 \tag{4}$$

with $\overline{P}_k$ the observed mean wet-day precipitation amount for the k-th class, $\hat{\mu}_k$ the expected mean wet-day precipitation amount from the fitted model, n_k the number of wet days, and CV_k the coefficient of variation for that class. The latter is estimated from the within-class variation. The value of D has to be compared with the percentiles of a chi-square variate with $K-p$ degrees of freedom, where p is the number of regression coefficients in the fitted model. Large values of D are indicative of lack of fit. The validity of the chi-square distribution may require pooling of classes, which is rather cumbersome when there are more than two predictor variables. The test was therefore not

considered in those situations. Further details about the goodness of fit test can be found in Brandsma and Buishand (1996).

Before fitting parametric models to the observed wet-day precipitation amounts, the relationships between P and other meteorological variables were explored by a nonparametric smoothing technique. A specific mathematical form is not assumed in that approach. The smooth curves help our eyes with the interpretation of a scatter plot and are useful to find suitable parametric formulations. The nonparametric smoother also provides additional diagnostics to check the adequacy of the fitted models. The technique used here is a generalisation of Cleveland's (1979) locally weighted running line or loess smoother for situations where the variance depends on μ as described by Hastie and Tibshirani (1990). The estimate of the function $g(T)$ at a target point T_0 is based on an IRLS fit of the linear model in Eq.(3) in a neighbourhood $N(T_0)$ of T_0. The size of $N(T_0)$ controls the smoothness of the fitted relationship. Small neighbourhoods result in a relatively rough curve. The fraction λ of points in $N(T_0)$ is known as the span of the smoother. Further details about the application of the loess smoother to precipitation relationships can be found in Brandsma and Buishand (1996).

When there are several predictor variables $X_1 = T, X_2, \ldots, X_p$ the model for the wet-day precipitation amounts takes the form:

$$P = \exp\left[g\left(X_1, X_2, \ldots, X_p\right)\right] + \varepsilon \tag{5}$$

In particular, we consider the case that $g\left(X_1, X_2, \ldots, X_p\right)$ is additive in the predictor effects:

$$P = \exp\left[a + g_1(X_1) + g_2(X_2) + \cdots + g_p\left(X_p\right)\right] + \varepsilon \tag{6}$$

For nonparametric regression, we need the additional assumption that $\mathrm{E}\left[g_i(X_i)\right] = 0$, $i = 1, \ldots, p$ to avoid free constants. The form of the functions $g_i(X_i)$ can be explored by the univariate loess smoother using the iterative backfitting algorithm (Hastie and Tibshirani, 1990). That algorithm also applies when the right-hand side of Eq.(6) contains linear terms like $a_i X_i$ and $a_j X_j$. In a parametric model for the amount of precipitation, each $g_i(X_i)$ is specified up to some unknown regression coefficients. The IRLS technique requires that the $g_i(X_i)$ are linear in these coefficients. The case that just one of the $g_i(X_i)$ in Eq.(6) is an arbitrary unspecified function is known as the semi-parametric model.

3. Inclusion of other meteorological information than temperature

We used daily mean sea level pressure (MSLP) data on a 5° latitude by 10° longitude grid to account for the effect of the atmospheric flow. This data set from the UK Meteorological Office was available for most of the Northern Hemisphere and extended back to 1880. From the MSLP data the following airflow indices were derived: (1) the direction of the flow; (2) the strength of the flow F; and (3) the total shear vorticity Z. The latter is a measure of the rotation of the atmosphere. Positive vorticity corresponds to a low pressure area (cyclonic) and negative vorticity corresponds to a high pressure area (anti-cyclonic). The MSLP grid was centred at 55°N-5°W for the British Isles and at 45°N-5°E for Switzerland and Italy. The Portuguese station Beja was not consid-

ered further in this study. Details about the calculation of the airflow indices are given in Jones et al.(1993).

For the Swiss stations the direction and strength of the flow are important airflow indices because of their influence on orographic precipitation enhancement. Vorticity is the most important airflow index for Durham and the Italian stations. For those stations the sea surface temperature needs to be considered as well.

3.1 Analysis of precipitation at Bern, Neuchâtel and Payerne

Bern, Neuchâtel and Payerne are located in western Switzerland at an altitude of ~500 m. For all three stations daily precipitation data were obtained for the period 1901-1993. Daily temperature data for that period were only available for Bern and Neuchâtel. For Payerne we used the temperature series of Bern, corrected for the difference in station elevation. The corrections ranged between 0.31°C for the months of May and June and 0.61°C for the month of January.

The data were divided in three categories of flow direction: (1) N/NE; (2) E/SE/S; and (3) SW/W/NW. Most rain (on average 64% for the three stations) comes from the SW-NW category. For Bern the P-T relationships for the three categories are presented in Fig. 2. The figure shows that for most temperatures, the mean precipitation amounts for the SW-NW category are about 1 to 2 mm higher than for the other two categories. The probability of precipitation is relatively small for the E-S category due to a screening influence of the Alps. For this category the mean daily precipitation amounts show the least variation with temperature. A strong increase of the mean daily precipitation with increasing temperature is found for the N/NE category.

For each category of flow direction the dependence of P on T and F was first explored with the nonparametric smoothing technique. Then parametric models were fitted to the observed relationships.

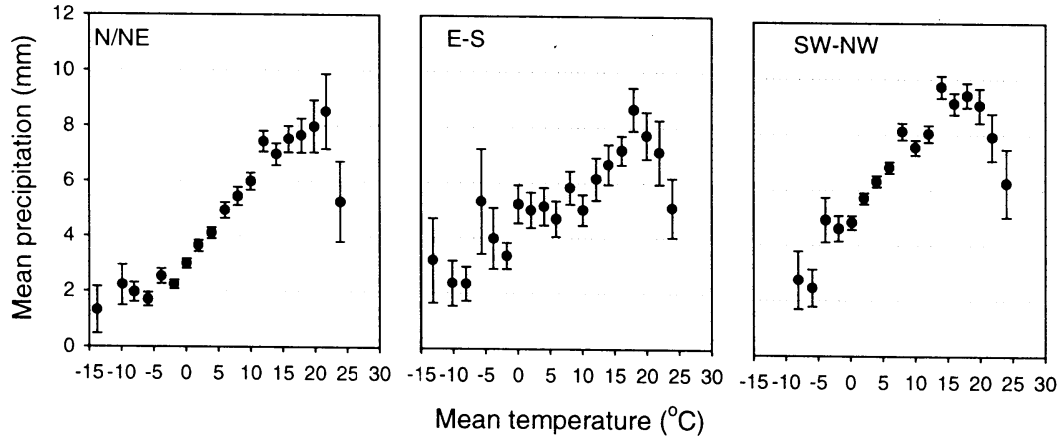

Figure 2: Relationship between daily mean precipitation and daily mean temperature for wet days (≥ 0.3 mm) at Bern for the period 1901–1993 for three categories of flow direction: (1) N/NE; (2) E-S; and (3) SW-N. The error bars give the standard error of the mean precipitation within each class.

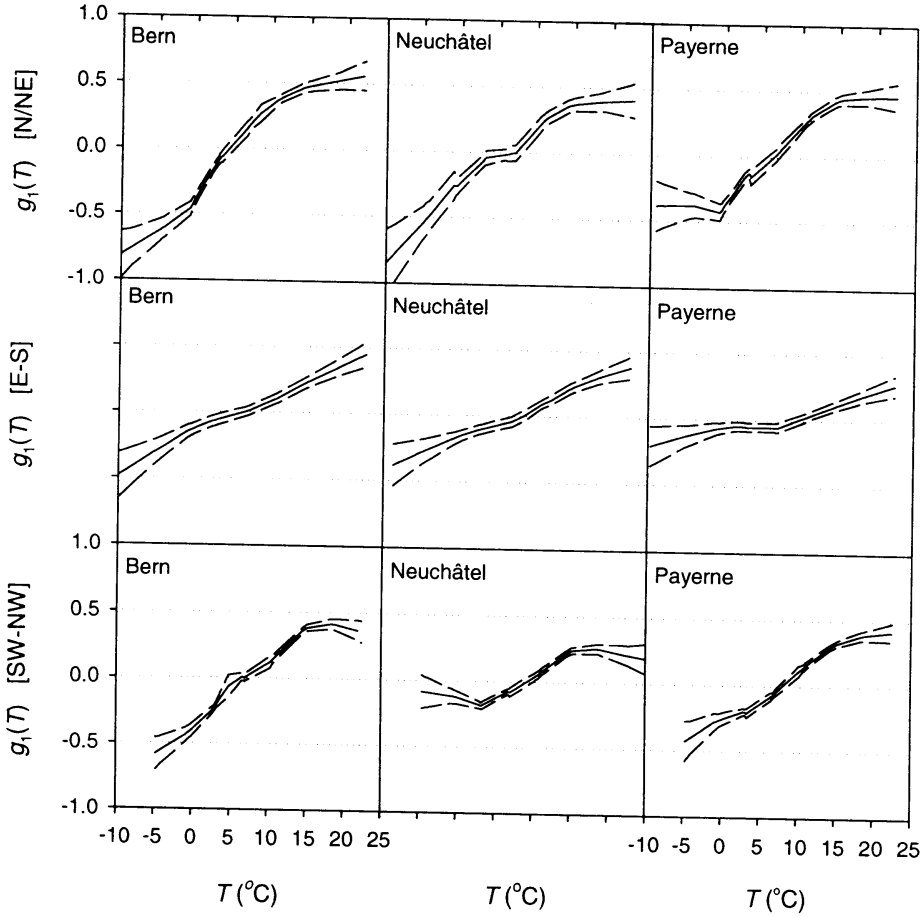

Figure 3: Estimates of the contribution $g_1(T)$ of temperature T to the logarithm of the expected daily amounts on wet days for Bern, Neuchâtel and Payerne, for three categories of flow direction. The dashed curves are pointwise 1 × standard-error bands (calculated according to Chambers and Hastie, 1993, pp. 303, 304).

Nonparametric fits

The nonparametric smoother assumes a model of the form

$$P = \exp[a + g_1(T) + g_2(F)] + \varepsilon \tag{7}$$

where $g_1(T)$ and $g_2(F)$ are smooth functions in T and F, respectively. The spans λ_T and λ_F for T and F were allowed to vary between 0.1 and 1.0 with intervals of 0.1. For each combination of spans we calculated the so-called Akaike-information criterion (*AIC*). The combination of λ_T and λ_F that gave the smallest *AIC* was considered further. To facilitate the comparison between the stations, we decided to use for all of them the same span for a specific category of flow direction. This combination consisted of the lowest λ_T and λ_F of the three stations. For the three categories of flow direction, this resulted in the following combinations of spans: (1) N/NE: $\lambda_T = 0.4$, $\lambda_F = 0.5$; (2) E-S: $\lambda_T = 0.7$, $\lambda_F = 0.9$; and (3) SW-NW: $\lambda_T = 0.4$, $\lambda_F = 0.5$.

Figures 3 and 4 present the estimated shapes of $g_1(T)$ and $g_2(F)$, respectively. From Fig. 3 it can be noted that there is in general an increase of $g_1(T)$ with increasing T. The resulting increase in P is generally smaller than in the P-T diagrams in Fig. 2 due to the inclusion of F. For the N/NE

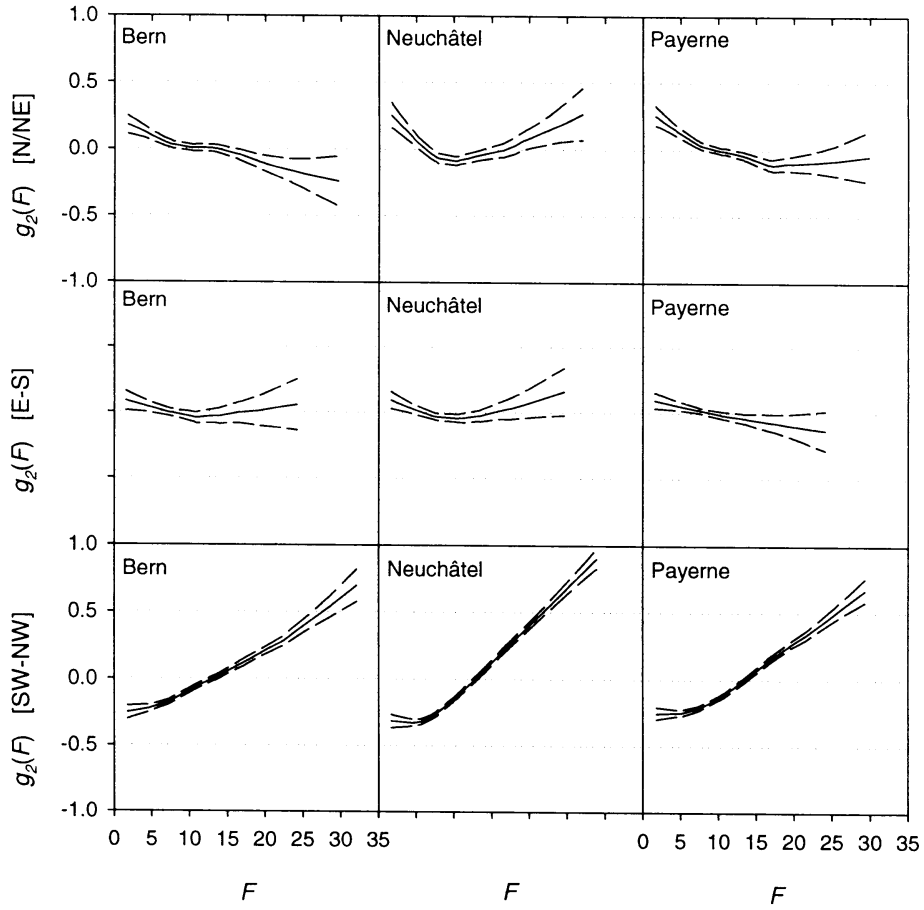

Figure 4: Estimates of the contribution $g_2(F)$ of strength of the flow F to the logarithm of the expected daily amounts on wet days for Bern, Neuchâtel and Payerne, for three categories of flow direction. The dashed curves are pointwise 1 × standard-error bands (Chambers and Hastie, 1993, pp. 303, 304); flow units are geostrophic, expressed as hPa per 10° latitude at 45°N (1 unit is equivalent to 0.87 m/s).

and SW-NW categories $g_1(T)$ is non-linear. The changes are relatively small at the upper end of the temperature range. For the SW-NW category the graph for Neuchâtel is rather different from that for Bern and Payerne. It is also apparent that for the E-S category $g_1(T)$ is almost linear.

Figure 4 shows for the SW-NW category a strong increase of $g_2(F)$ with increasing F. Possible explanations of this phenomenon are the enhanced supply of maritime air on days with a strong west circulation and a larger influence of the mountains on such days. However, $g_2(F)$ is almost constant at low values of F, especially for Neuchâtel and Payerne. For the N/NE category the relationship between precipitation and strength of the flow is less strong and more or less opposite to that for the SW-NW category. Besides, there are considerable differences between the three stations (for small values of F there is a decrease of $g_2(F)$ with increasing F, for Bern $g_2(F)$ continues to decrease while especially for Neuchâtel $g_2(F)$ starts increasing for larger values of F). A reversal of the effect on orographic rainfall has been reported elsewhere (Weston and Roy, 1994; Brown, 1995). The differences between the stations indicate that the local topography is important. For the E-S category the relationship between P and F is weak, which is probably caused by the fact that the stations are situated along the lee side of the Alps.

Parametric model

The non-linear effect of T on precipitation was modelled by a Natural Cubic Spline (NCS). An NCS with knots $s_1,...,s_q$ is a separate polynomial for each of the intervals $(s_1,s_2),...,(s_{q-1},s_q)$ and is linear outside (s_1,s_q). The different pieces are forced to join at these knots such that $g(T)$ itself and its first and second derivatives are continuous at each s_j and thus over the entire temperature range. These continuity constraints and the linearity for $T < s_1$ require that $g(T)$ is of the form:

$$g(T) = a + bT + \sum_{j=1}^{q} d_j (T - s_j)_+^3 \tag{8}$$

where $(T-s_j)_+ = \max(0, T-s_j)$. This equation contains $q + 2$ parameters. Linearity for $T > s_q$ leads to the following two parameter constraints:

$$\begin{cases} d_1 + d_2 + \cdots + d_q = 0 \\ d_1 s_1 + d_2 s_2 + \cdots + d_q s_q = 0 \end{cases} \tag{9}$$

It turned out that an NCS with four knots generally described the temperature effect quite well. The position of the knots was found by trial and error. Only minor improvement could be achieved when the position of the knots was optimised for each station and category of flow direction. Therefore, we chose to locate the knots for T at the same positions for all stations and categories of flow direction at 2, 7, 12 and 17 °C. We used a truncated linear term $(F - t_1)_+$ to represent the changes in the slope of the contribution of the strength of the flow for the N/NE (Neuchâtel, Payerne) and SW-NW (all stations) categories. Our complete parametric model takes the form:

$$P = \exp[g(T, F)] + \varepsilon \tag{10}$$

where

$$\begin{aligned} g(T, F) = a + bT + d_1 (T - s_1)_+^3 + d_2 (T - s_2)_+^3 + d_3 (T - s_3)_+^3 + d_4 (T - s_4)_+^3 \\ + e_1 F + e_2 (F - t_1)_+ \end{aligned} \tag{11}$$

with $(s_1,\ldots,s_4) = (2,7,12,17)$ and $t_1 = 7$ (SW-NW), 9 (N/NE, Neuchâtel) or 16 (N/NE, Payerne). Depending on the situation a number of terms could be left out in the final model. For the E-S category the model even reduced to the simple P-T relationship defined by Eqs.(1) and (3):

$$P = \exp(a + bT) + \varepsilon \tag{12}$$

Table 1 presents the parameter estimates of the final model and the values of the deviance statistic for the three stations and the three categories of flow direction. For Bern and Neuchâtel the values of D are significant at the 5% level for the N/NE and SW-NW categories. The large values of D for the SW-NW category are caused by a number of outliers. There is, however, no clustering of large positive and negative residuals that may suggest a systematic model deficiency. For the N/NE category, the model does not adequately describe the mean precipitation amounts for Bern and Neuchâtel at the lower end of the temperature range. However, this is of little interest for a precipitation scenario for a warmer climate. For Payerne there is no evidence of lack of fit.

Table 1: Estimates of the coefficients in Eq. (11), the deviance statistic D and the degrees of freedom df.

	Bern			Neuchâtel			Payerne		
	N/NE	E-S	SW-NW	N/NE	E-S	SW-NW	N/NE	E-S	SW-NW
a	1.295571	1.501876	1.420118	1.455661	1.504057	1.589376	1.320072	1.645614	1.443434
b	0.071505	0.028126	0.047836	0.043234	0.027312	–0.004352	0.037504	0.017833	0.019988
d_1	–0.000088	–	0.000148	0.000151	–	0.000563	0.000390	–	0.000401
d_2	–0.000188	–	–0.000677	–0.000761	–	–0.001641	–0.001452	–	–0.001231
d_3	0.000640	–	0.000911	0.001067	–	0.001595	0.001734	–	0.001261
d_4	–0.000364	–	–0.000382	–0.000458	–	–0.000516	–0.000672	–	–0.000430
e_1	–0.014253	–	–	–0.059550	–	–	–0.022825	–	–
e_2	–	–	0.033974	0.085528	–	0.055670	0.026330	–	0.040701
D	77.2*	44.7	95.7*	101.8*	44.3	85.0*	57.7	32.4	57.3
df	53	45	55	51	44	52	50	45	54

* Significant at the 5% level.

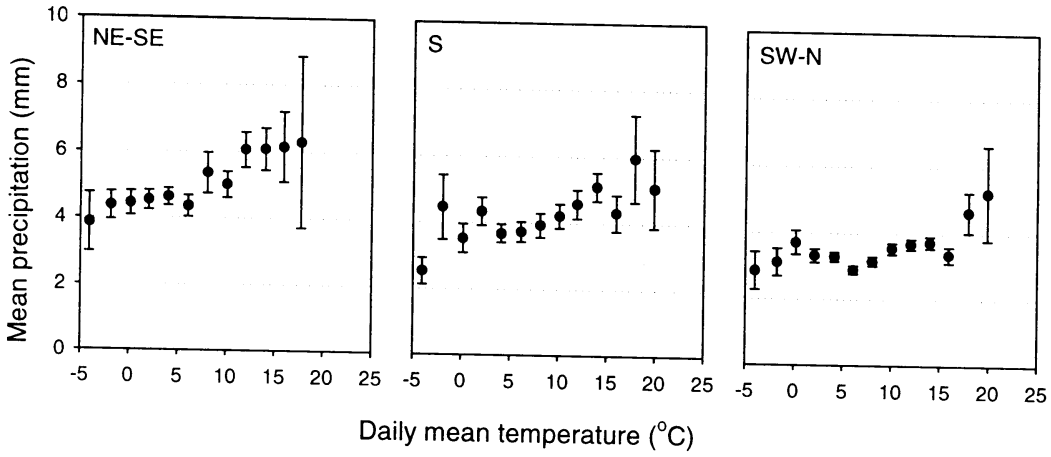

Figure 5: Relationship between daily mean precipitation and daily mean temperature for wet days (≥ 0.3 mm) at Durham for the period 1931–1990 for three categories of flow direction: (1)NE-SE; (2) S; and (3) SW-N. The error bars give the standard deviation of the mean precipitation within each class.

3.2 Analysis of precipitation at Durham

Durham is situated along the north-eastern coast of England at an altitude of 102 m. Daily precipitation and temperature data were obtained for the period 1931–1990. From Fig. 1 it is seen that the mean daily precipitation amount at Durham shows little variation with temperature. The mean amount is about 4 mm, independent of temperature. The P-T relationship has been examined further for three categories of flow direction: (1) NE/E/SE; (2) S; and (3) SW/W/NW/N. Figure 5 shows that the mean precipitation amounts in the NE-SE category are 1 to 2.5 mm higher than in the SW-N category for every temperature class (except for the highest temperature class). The differences can mainly be explained by the influence of the relatively warm North Sea for the NE-SE category (especially in the winter months) and the screening influence of mountains and hills for the SW-N category.

Nonparametric fits

We used nonparametric regression to explore the masking of the temperature effect for each category of flow direction separately. This effect could not be unmasked by the inclusion of the strength of the flow or the vorticity. Because England is surrounded by seas, we anticipated an effect of the sea surface temperature (*SST*) for all flow directions. Therefore, we decided to include the difference δ between land and sea surface temperature in our model:

$$\delta = T - SST \tag{13}$$

where T is on a daily and *SST* on a monthly basis. We first calculated the monthly *SST* on a 5° latitude × longitude grid from the *SST* anomalies in the Jones data set (Jones et al., 1991) and the *SST* climatology maps given in Bottomley et al. (1990). Subsequently, for each flow direction we averaged the monthly *SST* over two to four upstream grid cells. The local temperature T at Durham was used in Eq. (13). The difference between upstream air temperature and *SST* would have been a better predictor of the amount of precipitation. The required temperature data were, however, not available in this study.

In contrast to the Swiss stations, the vorticity Z is the most important flow characteristic for Durham (Conway and Jones, 1995). There is, however, also a significant effect of the strength of the flow F. The complete model for the nonparametric regression therefore reads:

$$P = \exp[a + g_1(T) + g_2(F) + g_3(\delta) + g_4(Z)] + \varepsilon \tag{14}$$

where $g_1(T)$, $g_2(F)$, $g_3(\delta)$ and $g_4(Z)$ are smooth functions in T, F, δ and Z, respectively. The spans λ_T, λ_F, λ_δ and λ_Z were all set equal to 0.5. We did not search for an optimum combination of the λs. The method followed for the Swiss stations becomes impracticable for more than two predictor variables. Moreover, the results for those stations showed that $\lambda = 0.5$ is often close to the optimal λ (in terms of AIC).

Figure 6 shows the estimated shapes of $g_1(T)$, $g_2(F)$, $g_3(\delta)$ and $g_4(Z)$. From the top row it can be noted that there is a clear, almost linear, increase of $g_1(T)$ with T. The strongest increase is found for the NE-SE category. The diagrams in the second row of Fig. 6 show that the shape of $g_2(F)$ differs for all categories. For the S and SW-N categories there is some analogy with the results for the E-S and N/NE categories for the Swiss stations (Fig. 4 upper and middle panels). The location along the lee side of mountains and hills may be an explanation for the relationships. On the other hand, for the NE-SE category there is some analogy with the SW-NW category for the Swiss stations (Fig. 4 lowest panels).

The representation of the effect of F meets serious difficulties for SW-N category. First, the effect is nonlinear and second, there are interactions with T, δ and Z. The latter implies that terms like FT, $F\delta$ or FZ should be considered. Especially the inclusion of the (F,T) and (F,δ) interactions meets difficulties because of the strong correlation between T and δ (correlation coefficient 0.82). The influence of those interactions on the estimated temperature effect is quantified below. Similar problems with interaction were met for the S direction category. However, the effect of F on P is small compared with other effects for this direction category. Therefore, we omitted F in the analysis for the S direction. From the diagrams in the third row of Fig. 6 it is seen that $g_3(\delta)$ decreases with increasing δ for all three categories. This is in line with the fact that in coastal areas a relatively warm sea (small δ) enhances precipitation, while a relatively cold sea has the opposite effect. Finally, the diagrams in the bottom row of Fig. 6 show that the shape of $g_4(Z)$ is non-linear, with a sharp increase for Z values up to about 50 geostrophic vorticity units and a nearly constant or even decreasing relationship for greater values of Z. The shape of $g_4(Z)$ is consistent with the empirical relationship between wet-day precipitation and Z for Durham in Conway et al. (1996).

Mixed parametric/nonparametric model

Figure 6 showed an almost linear increase of $g_1(T)$ with T. Because our main interest is in the effect of T on P, we decided to take $g_1(T)$ linear while the other terms remained arbitrary smooth functions:

$$P = \exp[a + bT + g_2(F) + g_3(\delta) + g_4(Z)] + \varepsilon \tag{15}$$

The function $g_2(F)$ is excluded for the S direction category. Table 2 presents the estimates of a and b for the three categories of flow direction together with their standard errors. The results for b imply that the increase in precipitation ranges between 3.0% per °C for the SW-N category and 4.9% per °C for the S category. These estimates are rather inaccurate. The standard errors are inflated by the correlation between T and δ. An interesting point is that omission of the terms $g_2(F)$ and $g_4(Z)$ in Eq.(15) has little effect on the estimate of b.

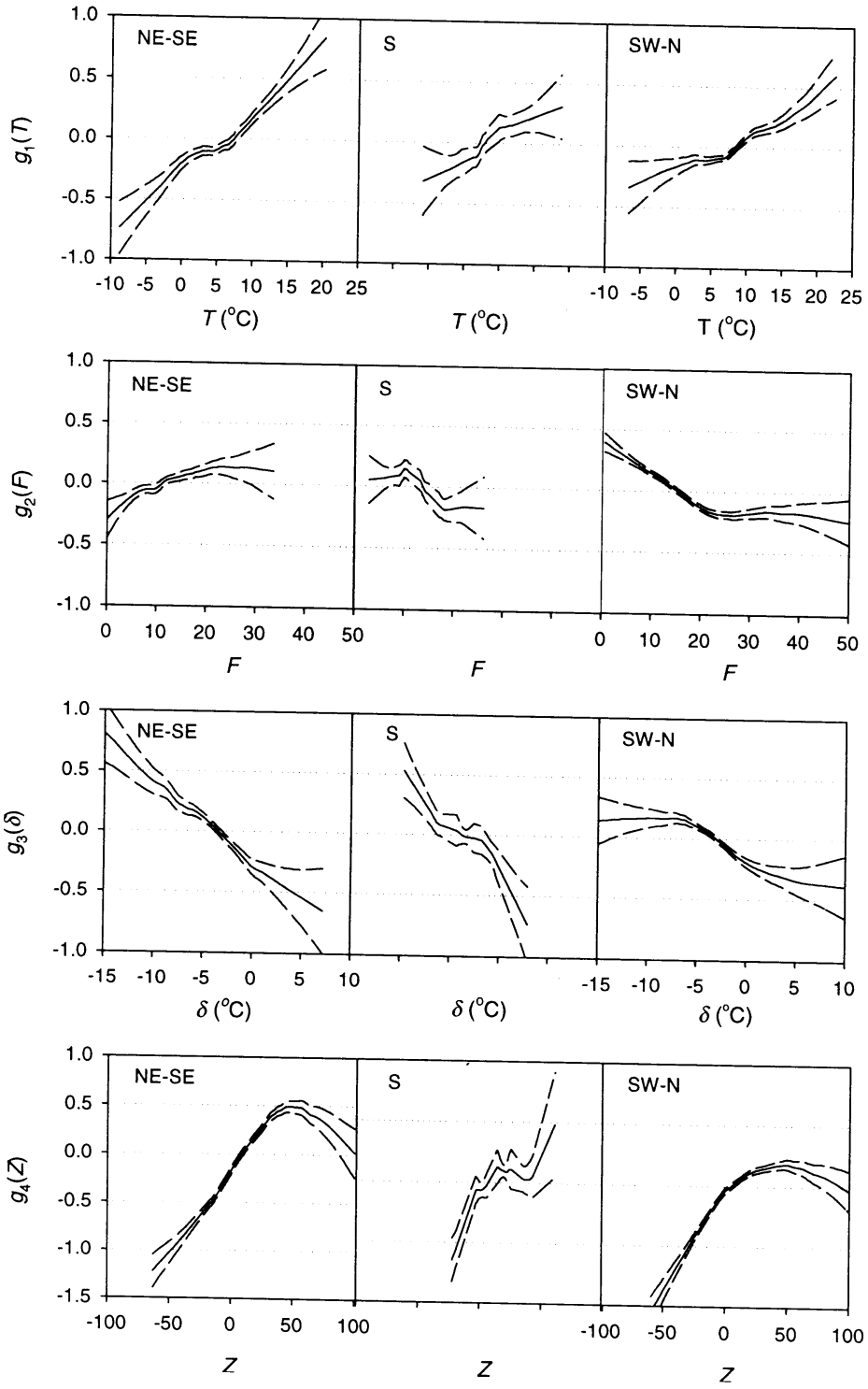

Figure 6: Estimates of the contributions $g_1(T)$, $g_2(F)$, $g_3(\delta)$ and $g_4(Z)$, of T, F, δ and Z, respectively, to the logarithm of the daily amounts on wet days for Durham, for three categories of flow direction. The dashed curves are pointwise 1 × standard-error bands (Chambers and Hastie, 1993, pp. 303, 304); flow and vorticity units are geostrophic, expressed as hPa per 10° latitude at 50°N (1 unit is equivalent to 0.73 m/s and 0.65×10^{-6} s^{-1} for flow and vorticity, respectively).

The (T,F) interaction for the SW-N category implies that the temperature effect for days with a strong SW-N flow differs from that with days with a weak flow. To quantify this difference, the data with $F < 15$ and $F \geq 15$ geostrophic flow units were treated separately (last two columns of Table 2). It appears that there is an important difference in the temperature effect for the two categories of flow strength. For $F < 15$ the precipitation increase is 3.4% per °C while for $F \geq 15$ the increase is only 2.3% per °C.

Table 2: Estimates of the parameters a and b in Eq. (15) for Durham. For the SW-N category, a and b are also given for $F < 15$ and $F \geq 15$ geostrophic flow units. The standard errors of the estimates are given between brackets.

	NE-SE	S	SW-N		
			all F	$F < 15$	$F \geq 15$
a	1.361 (0.0404)	1.049 (0.0768)	0.9881 (0.0451)	0.9511 (0.0704)	0.9236 (0.0780)
b	0.045 (0.0065)	0.048 (0.0097)	0.0304 (0.0057)	0.0338 (0.0073)	0.0225 (0.0095)

Applicability to other sites in England

To examine the variation of the P-T relationship over England, we analysed precipitation data from four other stations: Howick Hall (Northeast), Poaka (Northwest), Blackbrook (middle) and Windsor (South). Because daily temperatures were not available for those stations, we had to use alternative temperature series. For Howick Hall we took the daily temperature series of Durham and for the other stations the daily Central England temperature series (Parker et al., 1992). Figure 7 shows the P-T relationships of the four stations for wet days ($P \geq 0.3$ mm). Howick Hall is situated at the east coast, about 70 km to the north of Durham. Its P-T relationship resembles that for Durham (see Fig. 1). The other stations are much further away from

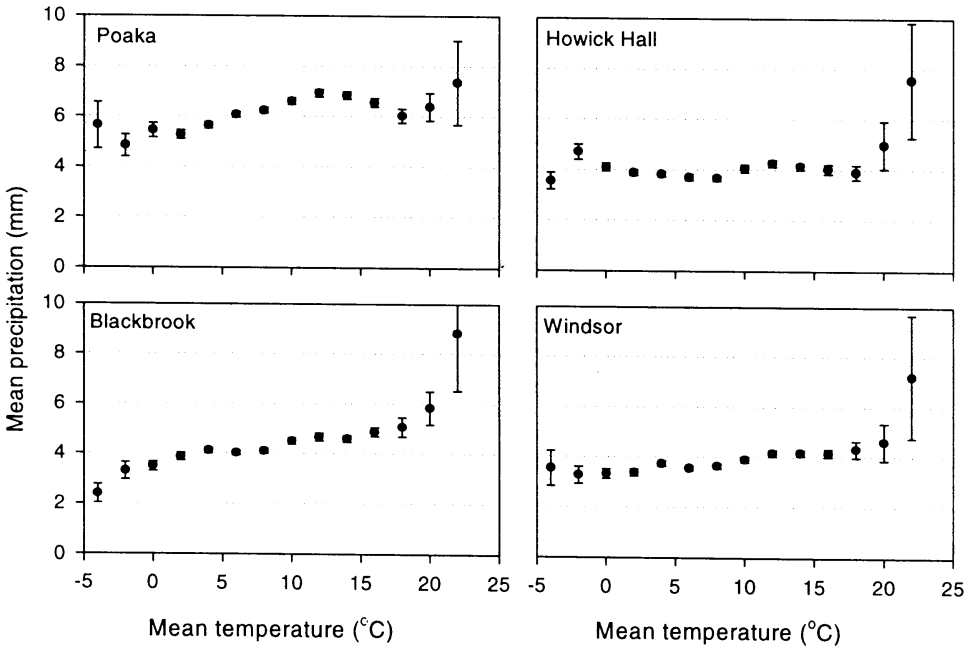

Figure 7: Relationship between daily mean precipitation and daily mean temperature for wet days (≥ 0.3 mm) at Poaka (1874–1988), Howick Hall (1901–1970), Blackbrook (1899–1988) and Windsor (1891–1988). The error bars give the standard error of the mean precipitation within each class. The total numbers of wet days for the four stations are 23674, 12459, 14429 and 16341, respectively.

Durham. Their graphs show more variation in daily mean precipitation than that of Durham and Howick Hall. At Blackbrook, which has the largest distance to the sea, there is a clear monotone increase in the mean amounts with increasing temperature.

For Howick Hall we carried out the same nonparametric analysis as for Durham. The shapes of $g_2(F)$, $g_3(\delta)$ and $g_4(Z)$ were the same as for Durham. The increase in precipitation ranged between 1.4% per °C for the SW-N category and 3.9% per °C for the S category, which is smaller than for Durham (Table 2). The standard errors of these estimates are nearly the same as for Durham.

3.3 Analysis of precipitation at Florence and Livorno

Florence and Livorno are both situated to the south-west of the Apennine mountain range in the north-western part of Italy at an altitude of 76 and 3 m, respectively. Daily precipitation and temperature data were obtained for the periods 1935–1987 for Florence and 1924–1941,1951–1979 for Livorno. Supplementary hourly data were obtained for the period 1962–1986. In Fig. 1 there is no clear relationship between daily precipitation and temperature at Florence. For temperatures between 5 and 30 °C the mean daily precipitation amount on rain days is about 8 mm, independent of temperature. The P-T relationships only slightly depend on flow direction, despite the barrier effect of the Alpine-Apennine range. A major factor influencing precipitation in Italy is the unstabilising effect of the Mediterranean Sea. This facilitates cyclogenesis in the vicinity of Italy.

Nonparametric fits

Because of the unstabilising effect of the Mediterranean Sea, we anticipated an effect of δ and Z on P. For Florence and Livorno the loess smoother was used to explore the effect of T, δ and Z on P. The value of δ was calculated in the same way as for Durham, except that we only considered one *SST* grid box in the vicinity of Florence and Livorno. The smoother assumes a model of the form:

$$P = \exp[a + g_1(T) + g_3(\delta) + g_4(Z)] + \varepsilon \tag{16}$$

where $g_1(T)$, $g_3(\delta)$ and $g_4(Z)$ are smooth functions in T, δ and Z, respectively. As for Durham, the spans λ_T, λ_δ and λ_Z were all set equal to 0.5.

Figure 8 shows the estimated shapes of $g_1(T)$, $g_3(\delta)$ and $g_4(Z)$ for Florence and Livorno. For both stations P is strongly positively related to T and Z. There is also a strong negative relationship with δ.

A much stronger positive effect of temperature on precipitation is obtained when the mean hourly amounts on rain days are regressed on T, δ and Z. Figure 9 shows the estimated shapes of $g_1(T)$, $g_3(\delta)$ and $g_4(Z)$ for Florence. The increase in the amount of precipitation is about 10.2% per °C versus 5.9% per °C for the daily data. The explanation for this discrepancy is that the rainfall duration on wet days decreases with increasing temperature. For instance, for a mean daily temperature of 5°C the mean rainfall duration on wet days equals about 8 hours while for a temperature of 20°C this is only 5 hours. In the analysis of the daily data we also take into account the dry hours on a wet day, whereas for the hourly data we only consider the wet hours. As a result,

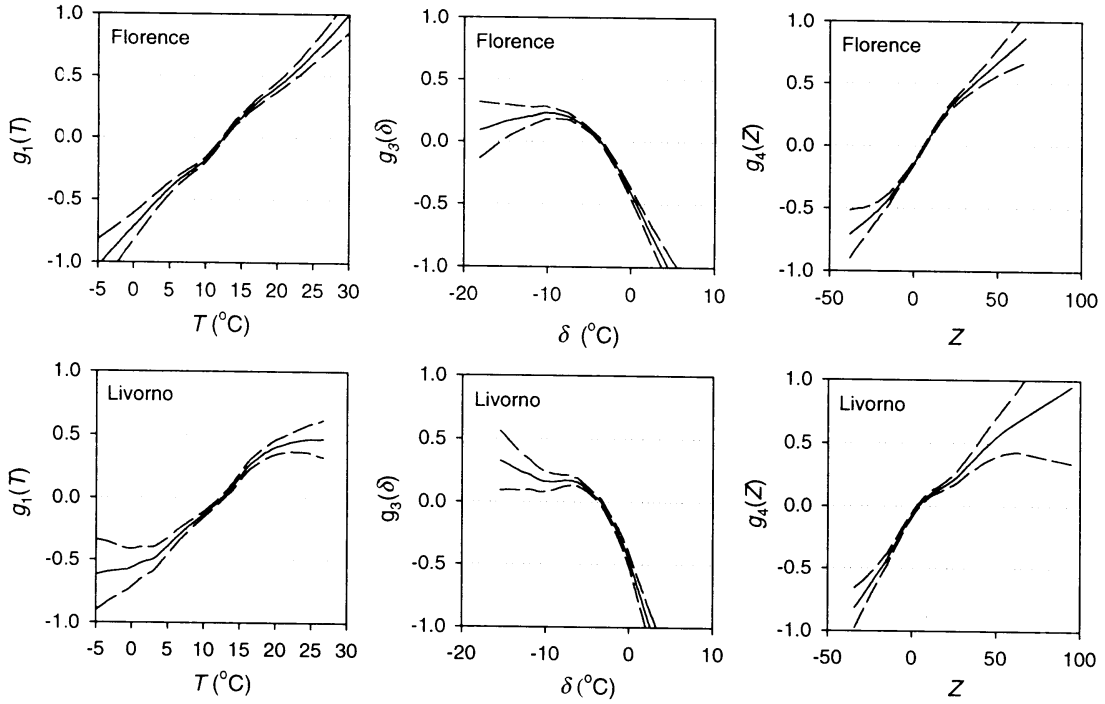

Figure 8: Estimates of the contributions $g_1(T)$, $g_3(\delta)$ and $g_4(Z)$, of T, δ and Z, respectively, to the logarithm of the expected daily amounts on wet days for Florence and Livorno. The dashed curves are pointwise 1 × standard-error bands (Chambers and Hastie, 1993, pp. 303, 304); vorticity units are geostrophic, expressed as hPa per 10° latitude at 45°N (1 unit is equivalent 0.78×10^{-6} s^{-1}).

the average rainfall intensity for the daily data increases less with increasing temperature in the present climate.

The shape of $g_3(\delta)$ for the mean hourly amounts differs from that in Fig. 8. This can be explained by the non-linear relation between δ and the number of rain hours on wet days (not shown). It is also seen that the increase of $g_4(Z)$ with increasing Z in Fig. 9 is much smaller than in Fig. 8. This is a result of the positive relation between Z and the number of rain hours on wet days (not shown).

Mixed parametric/nonparametric model

Figure 8 showed for Florence an almost linear increase of $g_1(T)$ with T. For Livorno the increase of $g_1(T)$ with T is slightly non-linear for $T < 5$°C and $T > 20$°C. As for Durham, we decided to take $g_1(T)$ linear while the other terms remained arbitrary smooth functions:

$$P = \exp[a + bT + g_3(\delta) + g_4(Z)] + \varepsilon \qquad (17)$$

Table 3 presents the estimates of a and b for Florence and Livorno together with their standard errors. The results for b imply that the increase in precipitation is 5.9% per °C for Florence and 5.2% per °C for Livorno.

	Florence	Livorno
a	1.384 (0.0602)	1.521 (0.0700)
b	0.057 (0.0049)	0.051 (0.0058)

Table 3: Estimates of the parameters a and b in Eq. (17) for Florence and Livorno. The standard errors of the estimates are given between brackets.

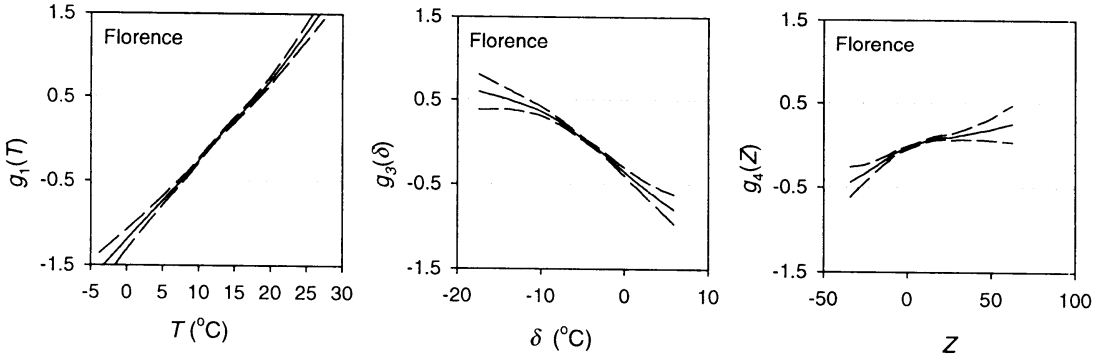

Figure 9: Estimates of the contributions $g_1(T)$, $g_3(\delta)$ and $g_4(Z)$, of T, δ and Z, respectively, to the logarithm of the expected mean hourly amounts on wet days for Florence. The dashed curves are pointwise 1 × standard-error bands (Chambers and Hastie, 1993, pp. 303, 304); vorticity units are geostrophic, expressed as hPa per 10° latitude at 45°N (1 unit is equivalent 0.78×10^{-6} s^{-1}). Note that the vertical scale differs from Fig. 8.

3.4 Discussion

In this section we studied the dependence of precipitation on temperature and other factors. For the Swiss stations we found distinct relationships for three categories of flow direction. T and F were the only two predictor variables. A point of concern is that at high temperatures the change in the mean wet-day precipitation amounts with increasing temperature is much smaller than that expected for summer thunder storms (Klein Tank and Können, 1994). To get a better description of the P-T relationship at high temperatures, it might be necessary to include some information about the precipitation mechanism.

As for the Swiss stations, we found for Durham distinct relationships for three categories of flow direction. Besides T and F we had to include the predictors vorticity Z and the difference δ between land an sea surface temperature. The inclusion of δ was crucial to unmask a positive relationship between P and T. However, δ is a rather rough measure of the effect of the sea surface temperature on precipitation. The strong positive correlation between T and δ has a negative impact on certain standard errors. Because both T and δ have to be included in the model, this problem cannot be avoided. Another important problem that remains are the interactions (F,T), (F,δ) and (F,Z) for the SW-N direction category. We dealt with these interactions by modelling the data for small and large F separately.

For Florence and Livorno it was not necessary to distinguish different categories of flow direction. T, δ and Z were meaningful predictor variables. As compared to the Swiss stations and Durham, the effect of temperature on precipitation is quite large. For the hourly data of Florence the temperature effect is even much larger. The explanation for this discrepancy is that the rainfall duration on wet days decreases with increasing temperature.

The question remains whether daily or hourly data must be used for precipitation scenario construction. If we use the relationship for the daily data in Fig. 8, it is implicitly assumed that the mean rainfall duration on wet days changes with temperature as in the present climate. In contrast, if we take the relationship for the hourly data in Fig. 9, it is implicitly assumed that the mean rainfall duration on wet days remains the same. Convection and frontal activity are important factors that determine the effect of temperature on rainfall duration. Higher temperatures are usually as-

sociated with increased convection, resulting in shorter and heavier rain storms. The assumption that the rainfall duration on wet days remains the same in a warmer climate is therefore not realistic. This complicates precipitation scenario construction on the basis of hourly data. We therefore prefer to use the daily data.

4. Seasonal variation of relationships

Up till now it has been assumed that the relationships between precipitation and other variables are constant over the year. The annual cycles of the predictor variables then determine the annual cycle in the mean wet-day precipitation amounts. Systematic differences between the observed monthly mean wet-day precipitation amounts and the expected monthly means from the annual cycles of the predictor variables are a first indication of a seasonally varying relationship. This point is addressed first. Then empirical relationships between anomalies are discussed. Anomalies are obtained by removing the annual cycle in the mean.

4.1 The annual cycle in the mean wet-day amounts

When the relationship between P and T is constant over the year, the expected monthly means are easily obtained by replacing the observed precipitation amount of each wet day by the mean amount in the appropriate temperature class (dots in Fig. 1). It is not necessary to specify the function $g(T)$. When there are several predictor variables, the expected monthly means follow similarly from the mean wet-day amounts in the various classes of these variables.

Figure 10 compares the observed mean wet-day amounts (dots) for Bern, Durham and Florence with those for (1) a constant relationship with T over the year (squares); and (2) for a constant relationship with T and the other predictors over the year (triangles). For Bern and Durham the latter also takes the different categories of flow direction into account. The observed mean wet-day precipitation amounts exhibit a clear annual cycle at Bern and Florence. For Bern this annual cycle is generally well reproduced in the two comparisons with the observed data. Only is the

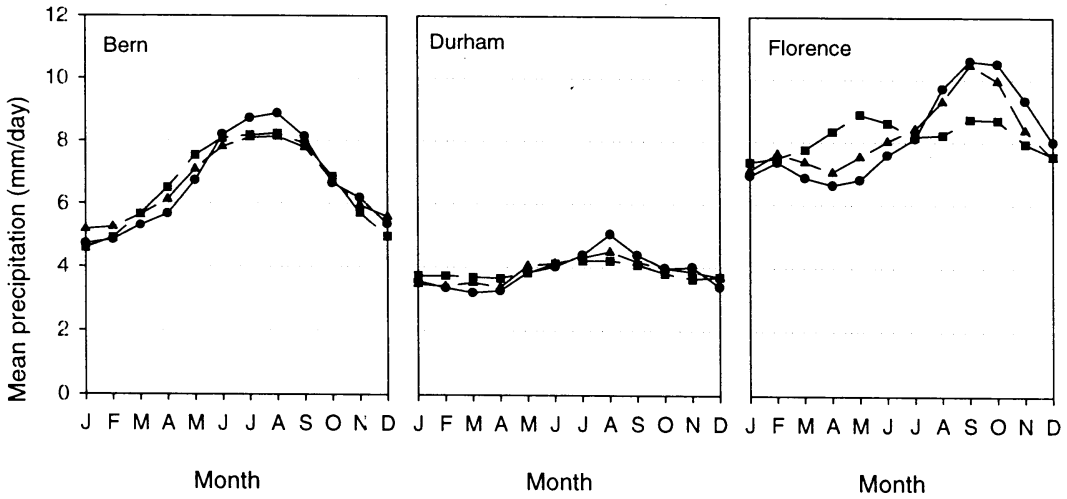

Figure 10: Seasonal variation of the monthly mean wet-day precipitation amounts for Bern, Durham and Florence. The dots refer to the observed mean wet-day amounts; the squares refer to the mean wet-day amounts obtained from a constant relationship with T; and the triangles refer to a constant relationship with T and the other predictors (see text).

mean wet-day precipitation amount somewhat underestimated in July and August and overestimated in spring. A similar discrepancy, although somewhat larger in magnitude, was observed by Klein Tank and Buishand (1993) for De Bilt. For Florence the annual cycle is not reproduced if only T or T and Z (not shown) are considered. The inclusion of δ is necessary to obtain a satisfactory reproduction of the seasonal cycle as shown in Fig. 10. The annual cycle of the observed precipitation amounts for Durham is weak. The mean wet-day precipitation amount is somewhat underestimated in August and overestimated in March.

4.2 Working with anomalies

Figure 11 shows for Bern, Durham and Florence the dependence between daily precipitation and temperature anomalies. Here, daily precipitation anomalies P' were obtained by dividing the daily amounts by their long-term means (relative anomalies), whereas the temperature anomalies T' refer to the differences between the daily wet-day temperatures and their long-term monthly means. The diagrams on the left in Fig. 11 refer to the whole year, those in the middle to the winter half year (October-March) and those on the right to the summer half year (April-September).

It appears that there is a marked difference between the diagrams for the year, the winter half year and the summer half year for the three stations. Consider for instance the diagrams for Bern. For most wet days T' is between –5 °C and +5 °C. In that temperature anomaly range the diagram for the year shows an almost linear increase in mean relative precipitation anomaly $\overline{P}'$ with increasing T' ($\approx$ 4.5% per °C). There is, however, no increase at high T'. The corresponding diagrams for the winter half year and the summer half year show marked differences. The relatively large change of $\overline{P}'$ with T' for the winter half year ($\approx$ 7% per °C) agrees with the observed increase in the mean wet-day precipitation amounts at low and moderate temperatures in Fig. 1 for Bern. Also, the diminishing of that increase at high temperatures is consistent with the relatively small change in $\overline{P}'$ for positive T' in the summer half year.

The diagrams for Durham are quite surprising because there is a negative relationship with T'. The influence of the sea surface temperatures is probably responsible for these results.

It is possible to account for both annual cycles and the atmospheric circulation by reducing the observed wet-day temperatures and precipitation amounts by their long term monthly means for distinct circulation types. Here, the objective Lamb scheme, initially developed by Jenkinson and Collison (1977), was used to classify the atmospheric circulation of each day. The scheme is based on the airflow indices in section 3. It distinguishes 26 weather types and an unclassified type. The resulting temperature and precipitation anomalies are denoted as T'' and P'', respectively. Figure 12 shows for Bern, Durham and Florence the mean relative precipitation anomalies $\overline{P}''$ as a function of T''. There is again a marked seasonal variation in the relationship between the anomalies. Another striking point is that the changes in mean precipitation in Fig. 12 are smaller than those in Fig. 11, in particular for Bern. For that station, the estimated temperature effect on precipitation is reduced by a factor of about 50% if allowance is made for the atmospheric circulation. This reduction in the temperature effect is larger than that in section 3.1 for the inclusion of F in the regression of the wet-day precipitation amounts. The difference must be ascribed to ignorance of seasonal variation in the regression models and to the methods used to account for the effect of the atmospheric circulation.

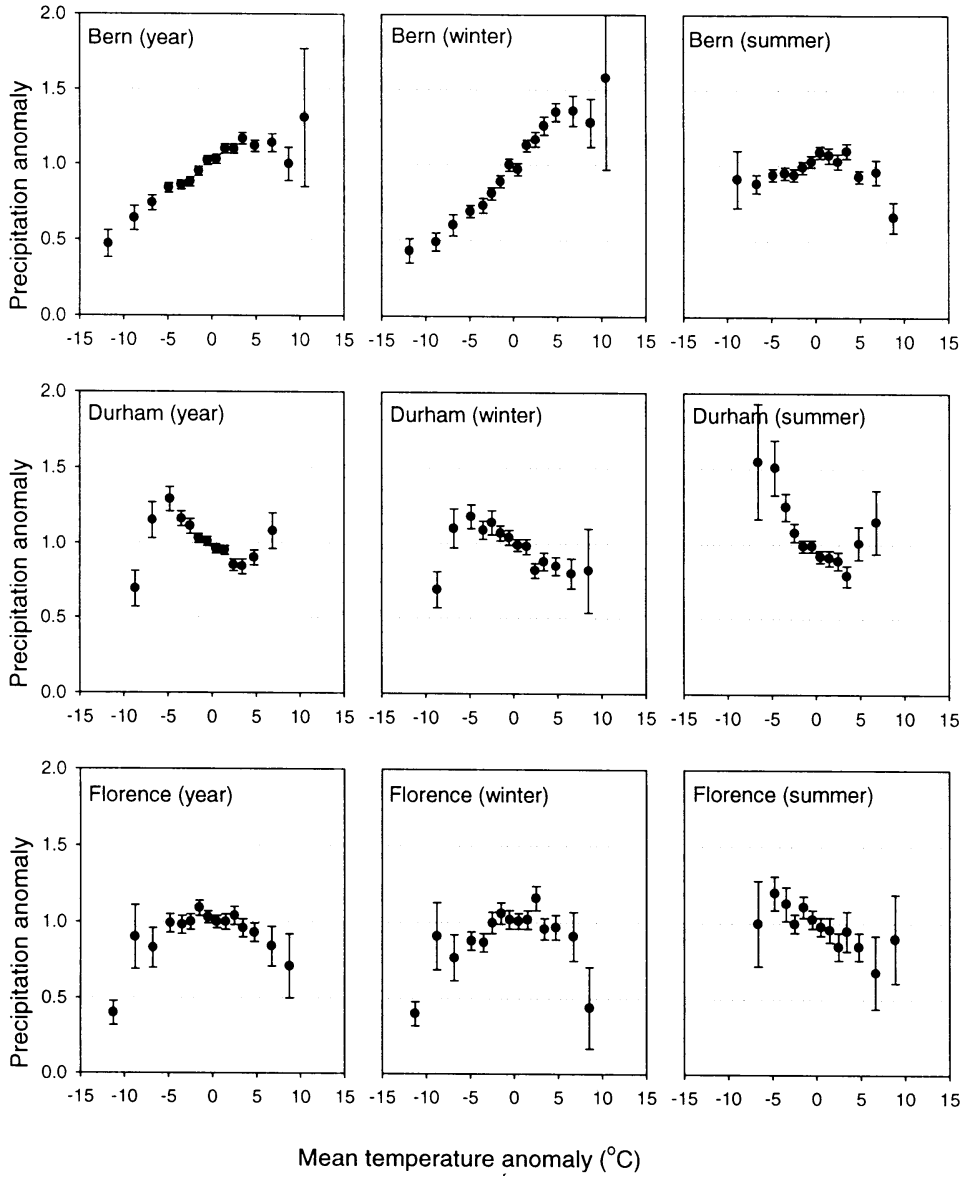

Figure 11: Relationship between daily mean relative precipitation anomaly $\overline{P}'$ and daily mean temperature anomaly T' for wet days (≥ 0.3 mm) at Bern (1901–1993), Durham (1931–1990) and Florence (1935–1987) for the whole year and the winter and summer half year. The anomalies were calculated by reducing the observed wet-day temperatures and precipitation amounts by their long term monthly means. The error bars give the standard error of the mean precipitation anomaly within each class.

The marked differences between the diagrams for the year, the winter half year and the summer half year for the three stations show that seasonal variation cannot simply be removed by analysing anomalies. The anomalies T'' and P'' also neglect interaction between temperature and the atmospheric flow as observed for the Durham data.

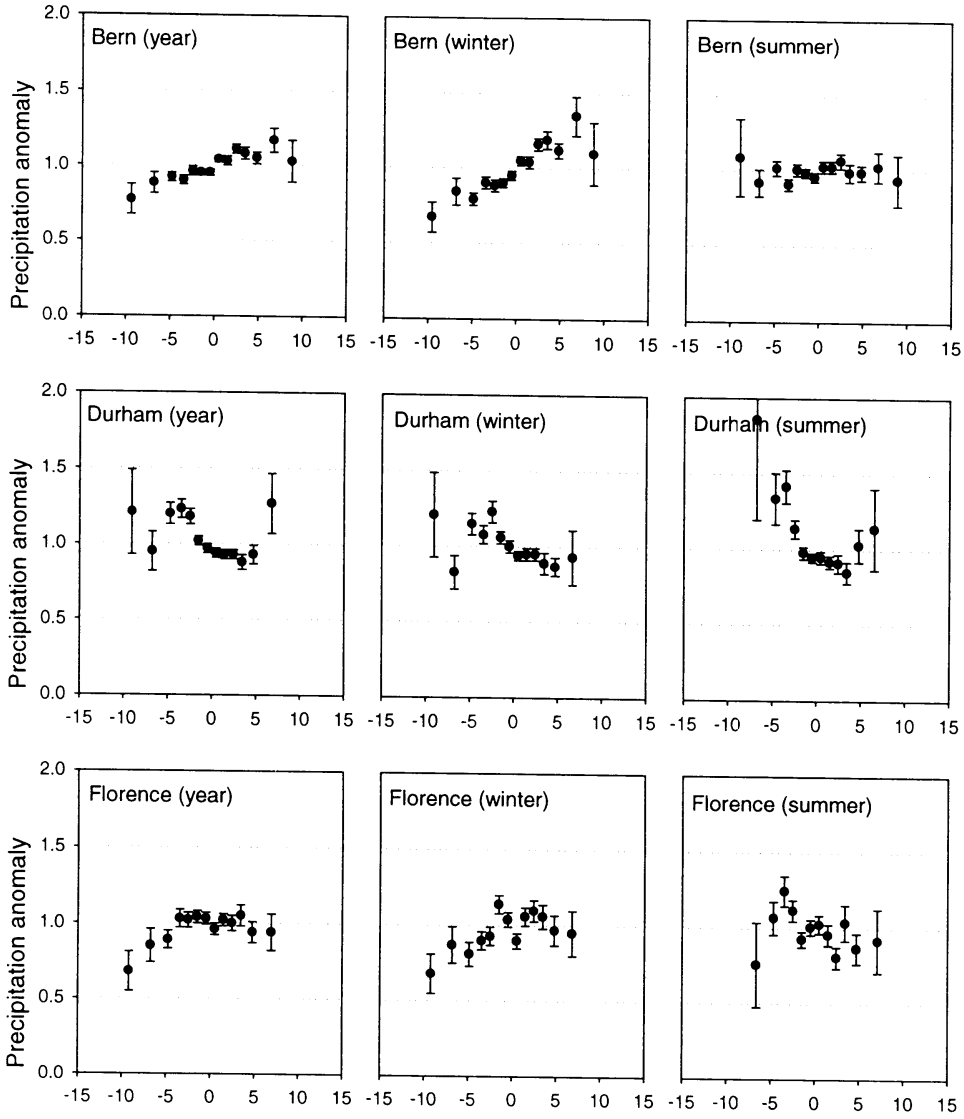

Figure 12: Relationship between daily mean relative precipitation anomaly $\overline{P}''$ and daily mean temperature anomaly T'' for wet days (≥ 0.3 mm) at Bern (1901–1993), Durham (1931–1990) and Florence (1935–1987) for the whole year and the winter and summer half year. The anomalies were calculated by reducing the observed wet-day temperatures and precipitation amounts by their long term monthly means for distinct circulation types (objective Lamb scheme). The error bars give the standard error of the mean precipitation anomaly within each class.

4.3 Discussion

It has been shown that the systematic differences between the observed monthly mean wet-day precipitation amounts and the expected monthly means from the annual cycles of the predictor variables are small. This does not necessarily imply that there is no seasonal variation in the relationships. Further study of the seasonal variation requires a separate analysis for each season. We

briefly examined the Bern data for the SW-NW directions for the standard 3-month seasons winter, spring, summer and autumn, showing some evidence of different relationships between P, T and F. However, there were also outliers as described in section 3.1, even in the case of a non-parametric fit. It was also not clear how seasonal variation could be described without a considerable increase in the number of parameters. Thus, incorporation of seasonal variation would lead to a complex model with evident lack of fit in this case.

5. Application to precipitation scenario production

The objective of the statistical linkage of daily precipitation to temperature, flow characteristics and sea surface temperatures was to provide precipitation scenarios for hydrological impact studies. This application requires that the fitted relationships continue to hold under the altered climate. The application further needs reasonable guesses of the changes in the predictor variables. One possibility is that the changes in the circulation patterns can be neglected, as in Matyasovszky et al. (1993), but that there is a homogeneous temperature rise over a large area. To generate daily precipitation sequences for a $2\times CO_2$ case, Matyasovszky et al. used the changes in the average height of the 500 hPa level to adjust the parameters of the daily precipitation distribution in a modified version of the model of Bárdossy and Plate (1992). The height of the 500 hPa level is strongly determined by temperature.

That the assumption of no changes in the circulation patterns may indeed be a realistic option for the changes due to increased greenhouse gases in the atmosphere is illustrated in Fig. 13. The figure gives the changes in temperature and flow characteristics over Switzerland (corresponding figures for England and Italy show almost the same features) in a simulation with the Hadley Centre coupled ocean-atmosphere model (Mitchell et al., 1995). Both greenhouse gases and the direct radiative effects of sulphate aerosols are represented in this simulation experiment. Up to the year 2050 there are no changes in the annual averages of the direction and strength of the flow and the vorticity. On the other hand, the increase in temperature is quite clear. After the year 2050 there is a small decline of the vorticity and the mean flow direction tends to shift from north-westerly to westerly. The changes in flow direction mainly occur during the winter half year.

In this section we first demonstrate how a precipitation scenario can be derived for the case of a spatially homogeneous warming. Then we discuss the complications that arise if there are changes in the flow characteristics as well. Some difficulties with the estimation of the temperature effect on precipitation are also identified.

5.1 Precipitation scenarios for the case of a spatially homogeneous warming

Here we deal with the case that there is a systematic change ΔT in the daily air and sea surface temperatures and that there are no changes in the flow characteristics. A quite reasonable assumption in this situation is that the number of wet days remains the same. For the sake of simplicity, we further assume that ΔT does not vary with season or flow direction. A precipitation scenario can then simply be obtained by multiplying the observed wet-day precipitation amounts by a scaling factor G. For models with additive predictor effects as those in Eq. (6), G is given by:

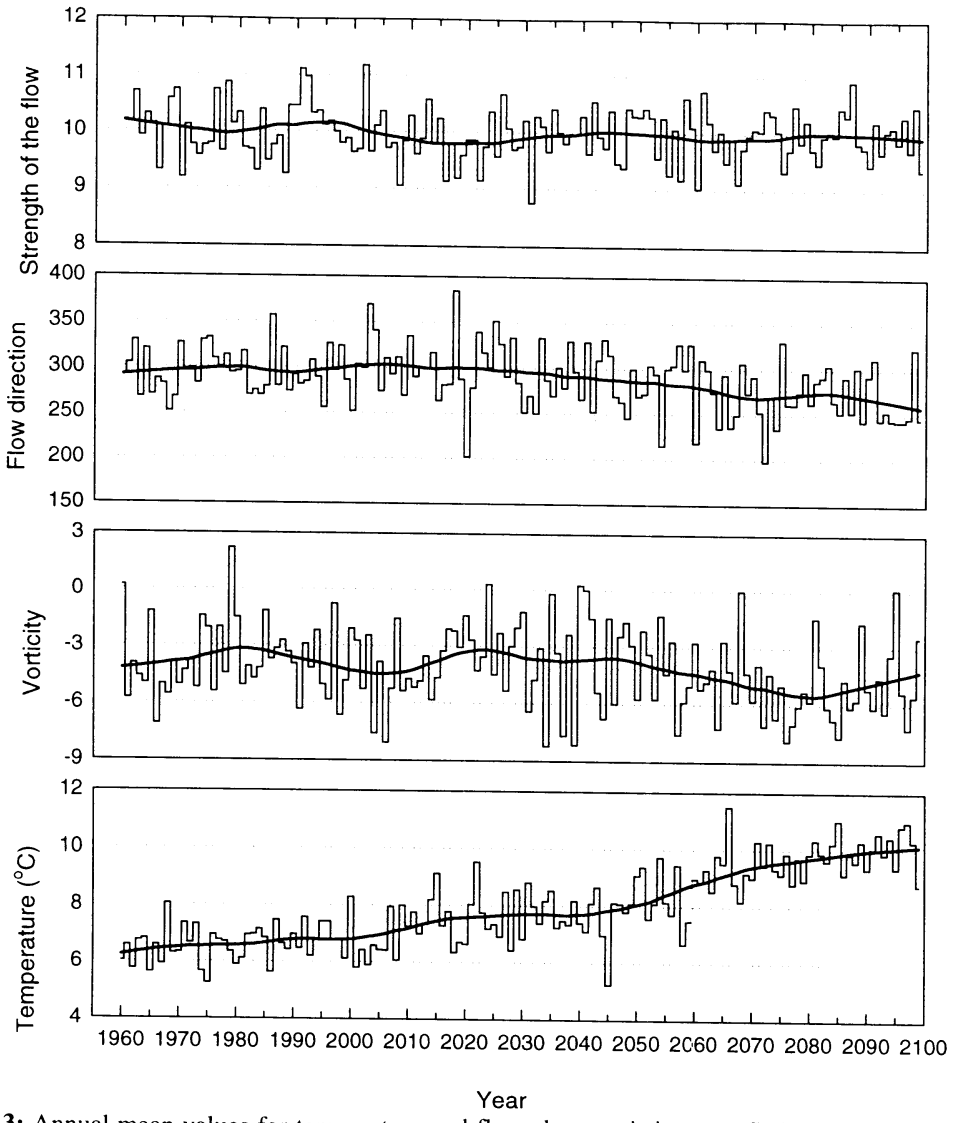

Figure 13: Annual mean values for temperature and flow characteristics over Switzerland in a simulation with the Hadley Centre coupled ocean-atmosphere model with aerosol effects included (Mitchell et al., 1995). Flow and vorticity units are geostrophic, expressed as hPa per 10° latitude at 45°N (1 unit is equivalent to 0.87 m/s and 0.78×10^{-6} s^{-1} for flow and vorticity, respectively). The solid lines are locally weighted running-line smooths with a span of 30 years.

$$G(T,\Delta T) = \exp\left[g_1(T+\Delta T) - g_1(T)\right] \tag{18}$$

The factor G generally depends on both ΔT and T. The dependence on T disappears if $g_1(T)$ is linear in T as in the mixed parametric/nonparametric models for Durham and the Italian stations in Eqs. (15) and (17), respectively.

A deterministic transformation of historical precipitation records implies that the temporal dependence of precipitation is more or less preserved as it should be when there are no significant changes in the atmospheric circulation. The transformation only requires a statistical description of the mean precipitation amounts instead of their complete distribution as in Matyasovszky et

al. (1993). The method proposed by those authors also needs a substantial extension for applications where daily temperature data are needed.

Table 4 presents the changes in the mean precipitation for Bern, Neuchâtel, Payerne, Durham, Florence, and Livorno for the year, the winter half year (October-March) and summer half year (April-September). The case Durham* refers to the model that dealt with the interaction between T and F for the SW-N category. It is seen from the table that the changes in the annual mean precipitation are generally greater than the changes predicted by GCMs (1.5–3% per °C) and smaller than the increase in maximum water vapour content (≈ 8% per °C). There are, however, considerable differences between the stations. For the Swiss stations, the increases in precipitation in the summer half year are much smaller than in the winter half year.

	Year	*Winter*	*Summer*
Bern	11.2	16.8	7.5
Neuchâtel	7.3	9.5	5.3
Payerne	9.5	12.7	7.1
Durham	11.1	11.4	10.9
Durham*	10.9	10.8	11.0
Florence	17.1	17.1	17.1
Livorno	15.3	15.3	15.3

Table 4: Precipitation changes (%) for a spatially homogenous warming of $\Delta T = 3$ °C for Bern, Neuchâtel, Payerne, Durham, Florence and Livorno. In Durham* the interaction between T and F for the SW-N flow direction category is taken into account. Precipitation changes are presented for the year, the winter (October-March) and summer (April-September).

5.2 Extensions for changes in the flow characteristics

A scaling factor similar to that in Eq. (18) can be derived to account for the effect of a systematic change of F or Z on the mean wet-day precipitation amounts. However, a simple transformation of the observed wet-day precipitation amounts is not sufficient for that case, because a change in F or Z will generally be accompanied by an increase or decrease in the number of wet days. Klein Tank and Buishand (1995) describe the use of logistic regression to include or remove wet days in an observed record.

A deterministic transformation of observed rainfall is not the most obvious method when the frequencies of the flow directions change as well. In that case, it may be advantageous to combine a stochastic time series model for generating daily rainfall sequences, conditional on the large-scale circulation, with the regression models developed in the present paper, to adjust the precipitation amounts for the higher expected temperatures. The derivation of the temperature effect on the precipitation amounts needs some care in that application. Part of the temperature rise after the year 2050 in Fig. 13 is due to the systematic change in the mean flow direction. This contribution to the temperature rise must be separated from the overall warming resulting from the increased atmospheric greenhouse gas concentrations.

5.3 Confidence in the estimated temperature effect

The use of the transformation technique in section 5.1 requires that the temperature effect on precipitation can be separated from other factors. Suitable climatic data for such a separation may not be available. Regression models with a limited number of parameters can only take the most important factors into account. On the other hand, a model with many predictor variables becomes intractable, in particular when the effects of these variables are non-linear and when there are interactions between these variables.

There are also uncertainties in the modelling of the non-linear temperature effect on precipitation. For instance, for Bern we found that the parametric fit for the SW-NW category could be improved by taking an NCS with six knots for the temperature effect. The estimated change in summer precipitation is sensitive to the chosen NCS. For a spatially homogeneous warming of 3 °C, the increase in the mean precipitation for the summer half year is only 4.1% for the NCS with six knots (compared with 7.5% for the NCS with four knots). Furthermore, the effect of this warming on the mean precipitation amounts at Neuchâtel and Payerne is smaller than that for Bern, especially in the winter half year (Table 4). Although the temperature effect on precipitation may vary over the region, the differences can also be due to simplifications in our approach.

The confidence in the estimated temperature effect might also be lowered because we ignored the seasonal variation in the model parameters and the scaling factor G. Another point of concern is that at high temperatures the change in the mean wet-day precipitation amounts with increasing temperature is smaller than expected for summer thunder storms, especially for the Swiss stations. The predicted changes in precipitation for Durham, Florence and Livorno are strongly determined by the inclusion of a rather rough measure of the effect of the sea surface temperature on precipitation.

6. Conclusions

In this part of the report we explored the P-T relationship as a basis for precipitation scenario production. Six stations were considered: Bern, Neuchâtel and Payerne in Switzerland, Durham in England and Florence and Livorno in Italy. We showed that the methodology originally developed for De Bilt can be extended to the aforementioned locations in Europe. In contrast with De Bilt, it was necessary to include additional predictor variables like air flow indices and sea surface temperature. For the Swiss stations, information about the direction and strength of the atmospheric flow F was incorporated. In addition, for Durham we also took into account the vorticity Z and the difference between land and sea surface temperature δ. Z and δ were also important for the Italian stations. The effects of flow direction and strength could be ignored for these stations.

We used a two step modelling approach in which we first considered a nonparametric model and subsequently a parametric or mixed parametric/nonparametric model. The nonparametric model gave a clear insight into the joint effects of T, F, δ and Z on the expected precipitation amounts on wet days. Parametric NCS were introduced as flexible tools to model the nonlinearities in the P-T relationships for the Swiss stations. Abrupt changes in the effect of F for those stations could be modelled by a truncated linear term. For Durham and the Italian stations we used a mixed parametric/nonparametric model in which the effect of T on P was taken to be linear while the effect of the other variables was described in the same way as in the nonparametric model.

Anomalies of daily precipitation and temperature have different relationships in the winter and summer half year. Considering anomalies is therefore not sufficient to remove the seasonal dependence of the relationships. A promising result is that the expected monthly mean wet-day precipitation amounts from the annual cycles in the predictor variables are quite close to the

observed monthly means. Nevertheless, a more extensive study of the seasonal variation of relationships is needed.

From the fitted relationships a scaling factor was derived to produce a precipitation scenario for the case of a systematic temperature change. The effect of a homogeneous temperature rise is a 2 to 6% precipitation increase per °C.

A combination with other models is necessary to use our relationships for scenario construction in situations where the temperature increase is accompanied by a systematic change in the air-flow. Information on the precipitation mechanism may be required to improve our estimates of the changes in precipitation at high temperatures. It may also be worthwhile to study the dependence of rainfall duration on temperature and the use of alternative predictors like moisture and vertical stability.

Acknowledgements

We thank H.R.A. Wessels for this help with the meteorological interpretation of the various P-T relationships and J.J. Beersma for comments on an earlier version. The daily rainfall and temperature data for Bern, Neuchâtel and Payerne were made available by the Swiss Meteorological Institute, Zürich. P.D. Jones kindly provided us the daily rainfall and temperature data for Durham, the daily Central England temperature series and the UK Meteorological Office gridded daily MSLP data. We thank the UK Meteorological Office for their permission to use the daily rainfall data for Howick Hall, Poaka, Blackbrook and Windsor. We are also grateful to P. Burlando for making the Florence and Livorno data available. The daily rainfall and temperature data for Beja were kindly provided by J. Corte-Real. The simulated temperatures and air flow indices in section 5 have been supplied by the Climate Impacts LINK project (Department of the Environment Contract PECD7/12/96) on behalf of the Hadley Centre and UK Meteorological Office. This research was in part supported by the EC Environment Research Programme (contract: EV5V-CT94-0510, Climatology and Natural Hazards).

References

Bárdossy, A. and Plate, E.J., 1992. Space-time model for daily rainfall using atmospheric circulation patterns, *Wat. Resour. Res.*, **28**, 1247–1259.

Boer, G.J., 1993. Climate change and the regulation of the surface moisture and energy budgets, *Clim. Dyn.*, **8**, 225–239.

Bottomley, M., Folland, C.K., Hsiung, J., Newell, R.E. and Parker, D.E., 1990. *Global Ocean Surface Temperature Atlas*, Meteorological Office, Bracknell, and Massachusetts Institute of Technology, Cambridge, Mass, 333 pp.

Brandsma, T. and Buishand, T.A., 1996. Statistical linkage of daily precipitation in Switzerland to atmospheric circulation and temperature, accepted for publication in *Journal of Hydrology*.

Brown, K.R., 1995. The effect of wind speed on orographic enhancement, *Weather*, **50**, 266–272.

Buishand, T.A. and Klein Tank, A.M.G., 1996. Regression model for generating time series of daily precipitation amounts for climate change impact studies, *Stochastic Hydrol. Hydraul.*, **10**, 87–106.

Chambers, J.M. and Hastie, T.J., 1993. *Statistical Models in S*, Chapman and Hall, London, 608 pp.

Cleveland, W.S., 1979. Robust locally weighted regression and smoothing scatterplots, *J. Am. Statist. Assoc.*, **74**, 829–836.

Conway, D. and Jones, P.D., 1995. The use of weather types and air flow indices for GCM downscaling, submitted to *Journal of Hydrology*.

Conway, D., Wilby, R.L. and Jones, P.D., 1996. Precipitation and air flow indices over the British Isles, submitted to *Climate Research.*

Hastie, T.J. and Tibshirani, R.J., 1990. *Generalized Additive Models*, Chapman and Hall, London, 335 pp.

Hulme, M., 1994. Validation of large-scale precipitation fields in general circulation models, In: M. Desbois and F. Désalmand (Editors), NATO ASI Series, Vol. I 26 *Global Precipitation and Climate Change*, Springer-Verlag Berlin Heidelberg, pp. 389–405.

IPCC (Intergovernmental Panel on Climate Change), 1990. *Climate Change: The IPCC Scientific Assessment*, J.T. Houghton, G.J. Jenkins and J.J. Ephraums (Editors), Cambridge University Press, Cambridge, UK, 365 pp.

IPCC (Intergovernmental Panel on Climate Change), 1992. *Climate Change 1992: The Supplementary Report to the IPCC Scientific Assessment*, J.T. Houghton, B.A. Callander and S.K. Varney (Editors), Cambridge University Press, Cambridge, UK, 200 pp.

Jenkinson, A.F. and Collison, F.P. 1977. *An initial climatology of gales over the North Sea*, Synoptic Climatology Branch Memorandum no. 62, Meteorological Office, Bracknell (unpublished). Available from the National Meteorological Library, Meteorological Office, Bracknell, UK.

Jones, P.D., Wigley, T.M.L. and Farmer, G., 1991.Marine and land temperature data sets: a comparison and a look at recent trends, In: M.E. Schlessinger (Editor), *Greenhouse-Gas-Induced Climatic Change: A Critical Appraisal of Simulations and Observations*, Elsevier, Amsterdam, pp. 153–172.

Jones, P.D., Hulme, M. and Briffa, K.R., 1993. A comparison of Lamb circulation types with an objective classification scheme, *Int. J. Climatol.*, **13,** 655–663.

Klein Tank, A.M.G. and Buishand, T.A., 1993. *Modelling daily precipitation as a function of temperature for climate change impact studies*, Scientific Report WR-93–02, KNMI, De Bilt, 34 pp.

Klein Tank, A.M.G. and Buishand, T.A., 1995. *Transformation of precipitation time series for climate change impact studies*, Scientific report WR-95–01, KNMI, De Bilt, 63 pp.

Klein Tank, A.M.G. and Können, G.P., 1994. The dependence of daily precipitation on temperature, In: *Proceedings of the eighteenth annual climate diagnostics workshop, Boulder, Colorado, November 1–5, 1993*, U.S. Department of Commerce, Springfield, VA, pp. 207–211.

Matyasovszky, I., Bogárdi, I., Bárdossy, A. and Duckstein, L., 1993. Space-time precipitation reflecting climate change, *Hydrol. Sci. J.*, **38**, 539–558.

McCullagh, P. and Nelder, J.A., 1989. *Generalized Linear Models*, 2nd ed, Chapman and Hall, London, 511 pp.

Mitchell, J.F.B., Johns, T.C., Gregory, J.M. and Tett, S.F.B., 1995. Climate response to increasing levels of greenhouse gases and sulphate aerosols, *Nature*, **376**, 501–504.

Parker, D.E., Legg, T.P. and Folland, C.K., 1992. A new daily Central England temperature series, *Int. J. Climatol.*, **12,** 317–342.

Weston, K.J. and Roy, M.G., 1994. The directional-dependence of the enhancement of rainfall over complex orography, *Met. App.*, **1**, 267–275.

PART II

Comparison of circulation classification schemes for predicting temperature and precipitation in the Netherlands[2]

1. Introduction

The large-scale atmospheric circulation is an important driving force of the surface climate. Not surprisingly, several attempts have been made to relate the atmospheric circulation to local weather. In general, the first stage is the classification of the atmospheric circulation and the second stage is the assessment of the relationship between the categories of the classification and the local weather elements.

In Europe the Grosswetterlagen (GWL) have been used for many decades (Hess and Brezowski, 1969; Gerstengarbe and Werner, 1993). This manual system classifies for each day the atmospheric circulation over Europe and the eastern part of the North Atlantic Ocean. Another well-known manual system is that of the Lamb Weather Types, which pertains to the British Isles (Lamb, 1972).

In the past twenty years there has been a growing interest in automated classification schemes, often indicated as objective schemes. Jenkinson and Collison (1977) devised objective rules to allocate the daily circulation for each day to one of the Lamb Weather Types, using mean sea-level pressure (MSLP) data on a rather coarse grid. The application of this objective scheme to other areas than the British Isles only requires a shift of the centre of the grid-point pattern to the area of interest. Another objective scheme is the P27 classification scheme of daily 500 hPa patterns over Europe (Kruizinga, 1978).

In this part of the report, we compare the GWL system, the objective Lamb and P27 classification schemes with respect to the estimation of temperature and rainfall in the Netherlands. Both daily and monthly values are dealt with. The performance of the classification schemes is measured with the mean-squared-error skill score. In section 2 we give some background of the three classification schemes. In section 3 the estimation of daily values is considered. The comparison based on monthly values is presented in section 4. A short discussion of the main results is given in section 5.

[2] A more extensive manuscript on this topic has been submitted to *International Journal of Climatology*.

2. Classification systems for the Netherlands

2.1 Grosswetterlagen

Over several decades, Franz Baur developed the GWL concept using surface pressure patterns and knowledge of the observed weather elements. A list of the 29 weather types in the present-day GWL system and their corresponding meteorological descriptions can be found in Hess and Brezowski (1969). The latter authors modified the system to include the upper-air data that became available after World War II. Gerstengarbe and Werner (1993) presented a catalogue of Grosswetterlagen extending from 1881 through 1992. Since 1949, the Grosswetterlagen have been determined using both surface and upper-air charts. Older Grosswetterlagen were derived from surface weather maps only.

During a Grosswetterlage, there is little change in the main features of the weather over Europe and the eastern part of the North Atlantic Ocean. Each Grosswetterlage usually lasts three days or more, after which there is a transition to another Grosswetterlage. Every day is assigned to one of the 29 Grosswetterlagen or an unclassifiable type. For convenience, the GWL system can be broken down into three general categories: zonal, meridional, and mixed.

Bárdossy (1994) developed objective schemes to classify the Grosswetterlagen from gridded 700 hPa heights. Both neural networks and fuzzy rule-based clustering were considered. For daily rainfall estimation the best results were obtained with the fuzzy rules. Nevertheless, the performance of this objective scheme was worse than that of the subjective GWL system. Further details about the classification of Grosswetterlagen by fuzzy rules can also be found in Bárdossy *et al.* (1995). Automated versions of the GWL classification are not considered here.

2.2 Objective Lamb classification scheme

The objective Lamb classification scheme was initially developed by Jenkinson and Collison (1977) for the British Isles. From daily MSLP data on a regular 5° latitude by 10° longitude grid, extending back to December 1880, they derived for each day the following airflow indices: (1) the direction of the flow; (2) the strength of the flow; and (3) the total shear vorticity. The latter is a measure of the rotation of the atmosphere. Positive vorticity corresponds to a low pressure area (cyclonic) and negative vorticity corresponds to a high pressure area (anticyclonic). The values of the three airflow indices determine the weather type of the day considered. The full classification distinguishes a total of 27 weather types: anticyclonic, cyclonic, 8 directional types, 16 hybrid types and one type denoted as undefined. It was shown by Jones *et al.* (1993), that the resulting scheme quite well reproduced the seasonal counts of the basic Lamb Weather Types.

An important advantage of the objective Lamb scheme is that it can be applied to other parts of Europe as well. As shown in Fig. 1, we centred the grid near the Netherlands at 55°N, 5°E to obtain representative airflow indices.

2.3 P27 classification scheme

The P27 classification scheme is an objective scheme developed at KNMI (Kruizinga, 1978, 1979). It is an example of an eigenvector-based classification scheme known as principal component analysis (PCA). The P27 scheme uses daily 500 hPa heights on a regular grid of 36 grid

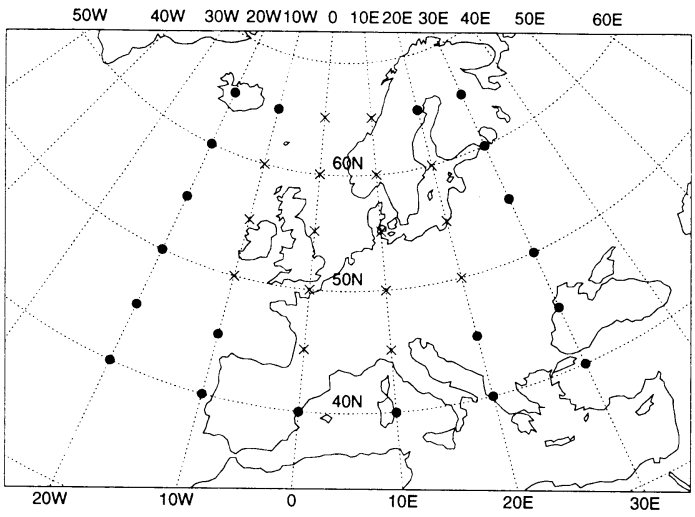

Figure 1: Grid used for the allocation of weather types in the objective Lamb scheme (crosses) and the P27 scheme (solid dots and crosses) for the Netherlands.

points as shown in Fig. 1, comprising nearly whole Europe. The actual 500 hPa height h_{tq} for day t at grid point q is reduced first by subtracting the daily average height $\overline{h}_t$ over the grid. This operation removes a substantial part of the annual cycle. The reduced 500 hPa heights p_{tq} are given by:

$$p_{tq} = h_{tq} - \overline{h}_t, \qquad q = 1,\ldots,36; \quad t = 1,\ldots,N \tag{1}$$

where N is the number of days. Subsequently, the vector $\mathbf{p}_t = (p_{t,1},\ldots,p_{t,36})^T$ of reduced 500 hPa heights is approximated as:

$$\mathbf{p}_t \approx s_{1t}\mathbf{a}_1 + s_{2t}\mathbf{a}_2 + s_{3t}\mathbf{a}_3, \qquad t = 1,\ldots,N \tag{2}$$

where $\mathbf{a}_1$, $\mathbf{a}_2$ and $\mathbf{a}_3$ are the first three principal component vectors (eigenvectors of the second-moment matrix of $\mathbf{p}_t$) and s_{1t}, s_{2t} and s_{3t} their amplitudes or scores. These amplitudes are calculated each day from the observed 500 hPa pattern. The flow pattern of a particular day is thus described by three amplitudes: s_{1t}, s_{2t} and s_{3t} instead of 36 grid-point values. It turns out that $s_{1t}\mathbf{a}_1$ characterises the east-west component of the flow, $s_{2t}\mathbf{a}_2$ the north-south component and $s_{3t}\mathbf{a}_3$ the cyclonicity (or anticyclonicity).

Using the first three principal components, the classification scheme is developed as follows. The range of each amplitude is divided into three equiprobable intervals. Then each pattern is, on the basis of its amplitudes, uniquely assigned to one of the 3x3x3=27 possible interval combinations.
A limitation of the P27 scheme is that the 500 hPa heights are available only since 1949.

3. Estimation of daily values

In this section we consider daily temperature and precipitation at De Bilt (52°6'N, 5°11'E) for the 1906–1993 period. The daily temperature is the average temperature of 24 hourly measurements. The daily precipitation refers to the 8–8 GMT interval. Besides the local precipitation,

we also examine the daily average amounts over the Netherlands. The country-wide averages are based on 12 stations, having good quality records for the 1907–1993 period. Both for the local and area-average values, a rainy day is defined as a day with a precipitation amount ≥ 0.3 mm.

We first compare the three classification schemes for the period 1949–1993. For the GWL and the objective Lamb scheme the relationships for that period are then used to estimate the daily values for the period prior to 1949.

3.1 Comparison for the period 1949–1993

For each circulation type of a classification scheme the long-term average temperature $\overline{T}_j$, precipitation $\overline{P}_j$ and the fraction f_j of rainy days were determined for January, February,..., December ($j = 1,...,J$ with J the number of circulation types in a classification scheme). These averages were used as an estimate of the daily temperature, precipitation and probability of rain. For a day with a circulation type j the prediction errors are: $T - \overline{T}_j$, $P - \overline{P}_j$ and $I_R - f_j$, with T the observed temperature, P the observed precipitation and I_R the indicator of rain, $I_R = 1$ if the day is wet and $I_R = 0$ if it is dry. Note that the prediction error $I_R - f_j$ is large on wet days with a low probabiltiy of rain and on dry days with a high probability of rain. A classification performs well if the prediction errors are small.

For all three classification schemes we present the mean-squared-error skill score S. This score gives the percentage reduction in the mean squared prediction error relative to that in the absence of the circulation classification. Some mathematical properties of this performance measure and its relationship to the correlation coefficient between the observed and estimated values are discussed in Buishand and Brandsma (1996).

Table 1 presents for the three classification schemes the seasonal and annual averages of S for temperature T, precipitation P and precipitation occurrence P_{oc}. The table shows that for T the objective Lamb classification scheme is inferior to the other classification schemes. Attempts to improve the skill for the objective Lamb scheme by choosing other class boundaries than those proposed by Jenkinson and Collison (1977) were not successful. For the GWL and the P27 classification scheme the results for the daily average temperature are similar to those in Kruizinga (1979) for the daily maximum temperature. From Table 1 it is further noted that for

Table 1: Mean-squared-error skill scores (%) for the predicted daily values in the period 1949–1993 for each of the three classification schemes. Seasons are standard three-month periods.

	Winter			Spring			Summer			Autumn			Year		
	GWL	Lamb	P27	GWL	Lamb	P27	GWL	Lamb	P27	GWL	Lamb	P27	GWL	Lamb	P27
Bilt															
T	48.6	36.7	41.9	39.2	25.6	43.3	40.8	31.4	51.7	29.7	21.2	28.9	39.6	28.7	41.5
P	20.1	23.4	19.6	13.3	17.2	12.7	13.6	15.0	11.1	17.3	21.6	20.6	16.1	19.3	16.0
P_{oc}	27.9	26.5	23.8	24.4	23.9	21.7	22.2	23.2	22.6	28.7	25.7	28.5	25.8	24.8	24.2
Neth															
P	25.2	29.2	24.7	18.7	23.3	17.8	21.1	24.4	19.4	25.4	29.5	30.1	22.6	26.6	23.0
P_{oc}	33.0	27.2	26.4	30.2	25.8	27.2	28.4	26.8	27.6	35.4	27.8	34.9	31.8	26.9	29.0

area-average precipitation a higher skill is achieved than for local precipitation. This was expected because the large-scale circulation is a very poor predictor of the local precipitation, particularly in convective situations, which occur most frequently in summer. Both for P and P_{oc} the increase in the percentage score for the daily area averages is of the order of 6%. For daily precipitation P in summer and autumn the increase is even somewhat larger. The improvement due to spatial averaging is relatively small for the prediction of rainfall occurrence with the objective Lamb scheme. Both for the local and area-average precipitation P the objective Lamb scheme performs somewhat better than the other classification schemes. The relatively good skill for the Lamb objective scheme is partly due to the sharp contrast between the average amounts on cyclonic and anticyclonic days.

3.2 Application to an independent verification set

The values of S in Table 1 may give a somewhat optimistic picture of the predictive skill of the classification schemes because they were calculated for the same period as the class averages. For the GWL and the objective Lamb scheme it is possible to calculate S for the period prior to 1949 using the 1949–1993 estimates of $\overline{T}_j$, $\overline{P}_j$ and f_j for each month and classification type. Still another possibility is to calculate the skill score for the period prior to 1949 using the 1907–1948 estimates of $\overline{T}_j$, $\overline{P}_j$ and f_j for each month and classification type. In the discussion below this skill score is denoted by $\tilde{S}$.

The values of S for the verification set are shown in Table 2. As expected, these values are lower than those in Table 1 for the calibration period. For the predicted temperatures from the GWL the difference in percentage score is on average even as large as 18%. The large decline in that case can partly be ascribed to the fact that the skill score $\tilde{S}$ for the temperatures in the period 1906–1948 is lower than the corresponding skill score for the period 1949–1993. Table 3 shows that the difference for the two periods is negative in 11 out of the 12 calendar months. This result is statistically significant at the 1% level according to the binomial distribution. The difference between the percentage scores in Table 3 is on average 6%. The lower performance for the data prior to 1949 and the earlier mentioned inferior results for the objective Lamb scheme suggest that the circulation characteristics at 500 hPa are better predictors of temperature than those near the surface.

Table 2: Mean-squared-error skill scores (%) for the predicted daily values in the verification period (1906–1948 for De Bilt, 1907–1948 for the Netherlands) for the GWL and the objective Lamb scheme.

	Winter		Spring		Summer		Autumn		Year	
	GWL	Lamb	GWL	Lamb	GWL	Lamb	GWL	Lamb	GWL	Lamb
Bilt										
T	33.6	27.2	18.3	17.6	26.5	27.5	7.8	11.7	21.5	21.0
P	10.1	8.8	5.2	9.9	2.8	7.4	12.2	10.7	7.6	9.2
P_{oc}	16.9	16.6	12.2	13.5	14.7	16.4	12.4	14.6	14.0	15.3
Neth										
P	18.2	15.6	10.3	18.4	6.1	15.5	19.3	18.5	13.5	17.0
P_{oc}	24.6	17.3	16.5	16.2	18.9	19.1	20.5	15.6	20.1	17.0

Table 3: Mean-squared error skill scores (%) for the predicted daily temperatures in the periods 1906–1948 ($\tilde{S}$) and 1949–1993 (S) for the GWL system.

	Jan	Feb	Mar	Apr	May	Jun	Jul	Aug	Sep	Oct	Nov	Dec	Year
1906–1948	45.6	43.7	25.5	27.1	31.6	35.9	41.6	30.4	22.6	28.7	25.2	40.1	33.2
1949–1993	53.7	49.7	40.1	41.1	36.3	43.1	43.4	35.8	26.1	25.3	37.6	42.4	39.6
Difference	–8.1	–6.0	–14.6	–14.0	–4.7	–7.2	–1.8	–5.4	–3.5	3.4	–12.4	–2.3	–6.4

For the objective Lamb weather types, the use of an independent verification set leads to a much smaller decrease in predictive skill for daily temperatures than for the GWL. Nevertheless, the scores $\tilde{S}$ for the period prior to 1949 are significantly lower than those for the period 1949-1993 (binomial sign test, 5% level). The average difference in percentage skill is only 2%.

Both for the GWL and the Lamb objective scheme the values of S for the precipitation characteristics in Table 2 are on average about 10% lower than those in Table 1. The skill score $\tilde{S}$ tends to be lower than the values in Table 1. The difference between the skill scores is in most cases statistically significant at the 5% level according to the binomial sign test. Systematic temporal changes in the relationships between precipitation and the weather types in the two classification schemes are partly responsible for the differences in predictive skill. Such changes may be long-term fluctuations of the precipitation characteristics within the weather types or may be associated with non-homogeneity of the data (observed precipitation, record of weather types).

A clear example of systematic temporal changes is presented in Fig. 2, which pertains to the area-average precipitation for the cyclonic days in the objective Lamb scheme. The smooth curves in this figure represent estimates based on a running weighted linear regression due to

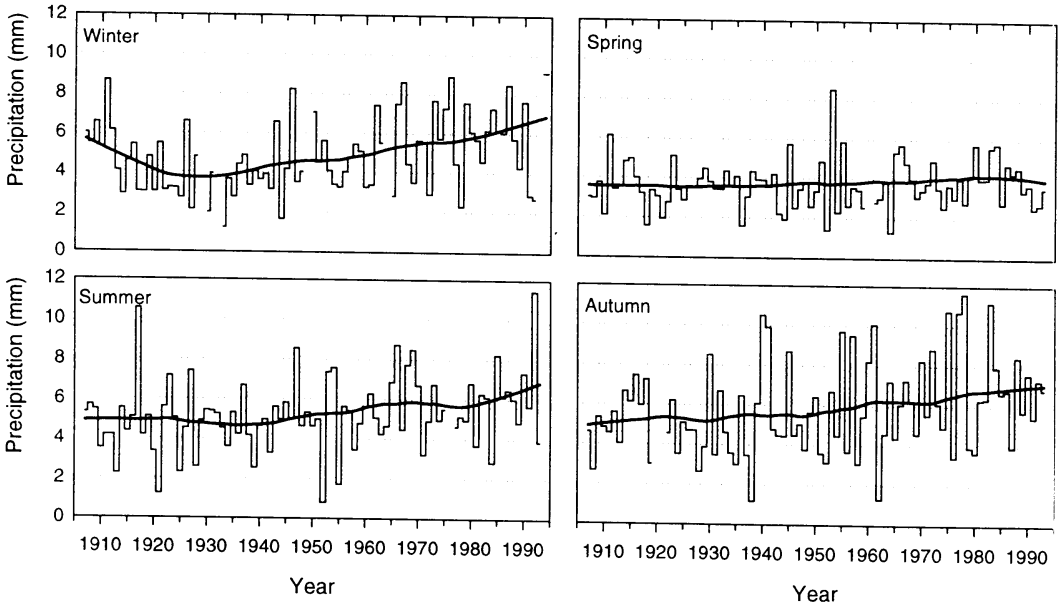

Figure 2: Area-average daily precipitation over the Netherlands on cyclonic days in the Lamb objective scheme for the period 1907–1993. The solid line is a weighted regression smooth using the data from the 30 nearest years in each year. Seasons are standard three-month periods with the winters dated by the year of January.

Cleveland (1979). The estimate for each year is derived from a weighted regression using the 30 nearest years. The weights decrease with increasing distance to the target point and are proportional to the number of cyclonic days in the year of interest. There is a rather strong change in the average daily precipitation on cyclonic days during this century in the winter season. Smaller, almost linear, changes are found for summer and autumn, whereas the spring season shows no apparent change. For winter, summer and autumn, the t-statistic for a linear trend is significant at the 1% level. The curve for the winter season, however, deviates from a straight line. The approximate F-test in Cleveland and Devlin (1988) indicates that this departure is significant at the 5% level. The rather large differences between the various seasons make it difficult to ascribe the changes in Fig. 2 to the non-homogeneity of the data. It should be noted further that temporal fluctuations in the frequency of occurrence also have some influence on the skill score. The skill score tends to be large for periods with a relatively high frequency of extreme weather types, i.e. weather types for which the precipitation characteristics strongly deviate from the overall average.

Weather types with a low frequency of occurrence can strongly influence the difference between S and $\tilde{S}$ (Buishand and Brandsma, 1996). Despite the rather large changes in mean rainfall in Fig. 2, the contribution of the cyclonic days to this difference does not dominate that of the other weather types. Further study shows that the differences between the skill scores in Tables 1 and 2 should be ascribed to changes of the mean temperatures and precipitation characteristics in more than one weather type.

The skill scores for P_{oc} in Table 2 are much lower than those attained with Model Output Statistics (MOS) weather forecasts in the Netherlands. The 1-day ahead forecast of rainfall occurrence at De Bilt has a percentage score of about 35% (Lemcke and Kruizinga, 1988). The MOS forecasts use logistic regression to relate the occurrence of rain to upper air characteristics. The better skill for these forecasts is mainly due to an appropriate choice of predictors for P_{oc}. The number of parameters in the logistic model is also much less than the number of classes in the weather classification schemes considered in this study, which makes it better suitable for prediction outside the period of calibration. In addition to the choice of other predictor variables, the incorporation of circulation characteristics on previous days or lagged dependent variables should be considered when there is serial correlation in the errors.

4. Estimation of monthly values

In this section we discuss the prediction of the monthly average temperatures, the monthly precipitation totals and the monthly number of rainy days from the daily weather types. Different methods can be used to predict monthly values (Buishand and Brandsma, 1996). Here we calculate the monthly values by averaging (T) or summing (P and P_{oc}) the estimated daily values for each month (cf. Bárdossy and Caspary, 1990).

We first compare the skill for the estimated monthly averages or totals for each of the three classification schemes for the period 1949–1993. We then examine the performance of these estimates for the GWL and the objective Lamb scheme for the period prior to 1949.

4.1 Comparison for the period 1949–1993

Table 4 presents for the three classification schemes the seasonal and annual averages of S for T, P and P_{oc}. For temperature, the relatively poor performance of the objective Lamb scheme is

Table 4: Mean-squared-error skill scores (%) for the predicted monthly values in the period 1949–1993 for each of the three classification schemes.

	Winter			Spring			Summer			Autumn			Year		
	GWL	Lamb	P27	GWL	Lamb	P27	GWL	Lamb	P27	GWL	Lamb	P27	GWL	Lamb	P27
Bilt															
T	69.8	52.1	61.5	55.6	38.2	62.1	48.1	40.3	63.1	55.1	37.8	54.7	57.2	42.1	60.3
P	59.5	57.4	57.9	50.4	51.8	48.1	37.7	33.6	38.1	44.9	46.1	47.0	48.1	47.3	47.8
P_{oc}	70.9	65.3	62.9	70.4	61.9	54.8	53.7	54.0	60.7	65.7	51.8	56.7	65.2	58.3	58.8
Neth															
P	65.2	62.6	61.4	61.1	59.6	55.6	53.3	48.0	52.4	59.2	57.5	58.1	59.7	56.9	56.9
P_{oc}	66.8	53.5	50.3	67.5	53.6	56.8	56.6	55.9	61.5	69.7	47.7	60.5	65.1	52.7	57.3

evident. This is partly caused by differences between the variances of the estimated monthly temperatures. For the monthly temperatures from the objective Lamb scheme the variance is only half that from the GWL. This comparatively low variance can be attributed to two different causes. First, the relatively poor performance of the objective Lamb scheme for the daily temperatures implies that the variance of the daily temperature estimates is relatively low (Buishand and Brandsma, 1996). Second, the persistence of the objective Lamb weather types is weaker than for the GWL, because in the subjective scheme the allocation of weather types is also affected by the atmospheric circulation on preceding and successive days. It was already noted in section 2.1 that in the GWL system one tries to achieve that the selected weather types have a duration of three days or more. The average run-length of the major weather types in this system ranges between 4 and 5 days. In the objective Lamb scheme all weather types have an average run-length less than 2 days.

For the monthly rainfall totals the three classification schemes perform almost equally well. Spatial averaging leads to a marked improvement of the predictive skill. For each of the three classification schemes the increase in percentage score is on average about 10%. According to the skill scores in Table 4 the GWL system provides better predictions of the number of rainy days in winter, spring and autumn than the other classification schemes. The effect of spatial averaging on the skill score is for P_{oc} less apparent than for P.

It is further noted that the percentage scores in Table 4 for the monthly values are larger than those for the daily values in Table 1. This is because the weather types not only explain a part of the daily variance, but also a part of the autocorrelation of the daily values. The increase in percentage score is on average 17% for temperature and 34% for the precipitation characteristics. The relatively small increase for temperature is due to the rather strong remaining autocorrelation in the prediction errors of the daily values. The lag 1 autocorrelation coefficient of these errors is about 0.6.

4.2 Application to an independent verification set

For the GWL and the objective Lamb scheme the class averages for the period 1949–1993 can be used to predict the monthly totals or averages for the data prior to 1949.

The seasonal and annual averages of S are shown in Table 5. The values of S are systematically lower than those in Table 4 for the calibration period. The largest differences are found for the monthly predictions based on the GWL. The average decline in percentage score of 19% for the

Table 5: Mean-squared-error skill scores (%) for the predicted monthly values in the verification period (1906–1948 for De Bilt, 1907–1948 for the Netherlands) for the GWL and the objective Lamb scheme.

	Winter		Spring		Summer		Autumn		Year	
	GWL	Lamb	GWL	Lamb	GWL	Lamb	GWL	Lamb	GWL	Lamb
Bilt										
T	54.6	43.6	29.9	32.0	48.0	41.9	20.7	18.8	38.3	34.1
P	40.6	38.7	22.4	27.5	29.2	32.4	56.2	46.1	37.1	36.2
P_{oc}	44.0	55.5	34.3	46.1	43.6	48.5	39.7	56.3	40.4	51.6
Neth										
P	50.3	44.2	31.6	41.9	26.4	35.2	59.1	53.7	41.9	43.7
P_{oc}	56.6	47.5	38.9	41.1	44.7	43.1	56.2	49.4	49.1	45.3

monthly temperatures is comparable to that for the daily temperatures. For the number of rainy days at De Bilt the average decline is even 25% for the GWL.

For the number of rainy days at De Bilt, correlation between the prediction errors of daily precipitation occurrence partly explains the spectacular decrease in percentage skill for the GWL classification in the verification period. The stronger correlation of the prediction errors in the verification period leads to a substantial reduction of the mean-squared-error skill score.

5. Discussion and conclusions

We have studied the prediction of daily and monthly values of temperature and precipitation using the long-term daily averages of these elements for distinct weather types. Three classification schemes were compared for the 1949–1993 period: the subjective GWL, the objective Lamb scheme and the objective P27 classification. For most seasons these classification schemes explain 15 to 30% of the variance of daily precipitation characteristics, 30 to 40% of the variance of the daily temperatures, and 40 to 60% of the variance of the monthly values of these elements. Especially for the GWL spectacular declines in predictive skill were found when the 1949-1993 averages were used to predict the values prior to 1949. Part of these declines must be attributed to systematic changes in the relationships between the observed local weather and the weather types. In particular, there is a strong indication that the introduction of upper-air charts has markedly improved the predictive skill of the GWL for temperature since 1949.

The objective Lamb scheme performs relatively poor for temperature. This is possibly due to the non-use of upper-air data in that scheme.

The three classification schemes perform better for area-average precipitation over the Netherlands than for local precipitation. It further turns out that for the prediction of the monthly area-average precipitation over the Netherlands the average of the vorticity index in the Lamb objective scheme does at least as well as the monthly amount obtained from the class averages in the full classification. Conway and Jones (1995) obtained a similar result for precipitation in Northeast England. Results of Wilby *et al.*(1995) for the British Isles indicate that inclusion of frontal information may significantly improve the estimation of annual rainfall over large areas. The experience from MOS weather forecasting shows that better predictions of daily rainfall occurrence at De Bilt are possible than those discussed in this paper.

Prediction based on the daily class averages is reasonable when there is no autocorrelation in the errors. Especially for the daily temperatures, this condition is not met. Information about the situation on the previous day (or days) must be included to improve the description of autocorrelation properties of the daily temperatures. The use of continuous airflow indices and other variables instead of binary weather type indicators is an other point of interest. It should be noted, however, that the relationships between daily precipitation characteristics and atmospheric flow indices are often non-linear (Conway *et al.*, 1995; Brandsma and Buishand, 1996). There may also be interactions between the effects of two different indices. Corte-Real *et al.*(1995) applied Multivariate Adaptive Regression Splines (MARS) to account for non-linearity and non-additivity in the relationships between monthly precipitation in Portugal and the large-scale circulation for the winter season. Autocorrelation, extreme non-normality of daily precipitation and dependence of the variance on the flow characteristics prevent the use of this technique to daily values. The large sample size in case of daily data may also put limitations on the use of MARS.

Acknowledgements

The authors are grateful to P.D. Jones (Climatic Research Unit, University of East Anglia, Norwich) for suggesting this study and for providing the UK Meteorological Office gridded MSLP data. They also thank J.J. Beersma, A.J. Coops and H.R.A. Wessels for comments on earlier versions. The research was in part supported by the EC Environment Research Programme (contract: EV5V-CT-94-0510, Climatology and Natural Hazards).

References

Bárdossy, A. 1994. *Modelle zur Abschätzung der regionalen hydrologischen Folgen einer Klimaänderung*, Mitteilungen 47, Institut für Hydrologie und Wasserwirtschaft Universität Karlsruhe, Karlsruhe, Germany, 90 pp. (in German).

Bárdossy, A. and Caspary, H.J. 1990. Detection of climate change in Europe by analyzing European circulation patterns from 1881 to 1989, *Theor. Appl. Climatol.*, **42**, 155–167.

Bárdossy, A., Duckstein, L. and Bogárdi, I. 1995. Fuzzy rule-based classification of atmospheric circulation patterns, *Int. J. Climatol.*, **15**, 1087–1097.

Brandsma, T. and Buishand, T.A. 1996. Statistical linkage of daily precipitation in Switzerland to atmospheric circulation and temperature, accepted for publication in *J. Hydrol.*

Buishand, T.A. and Brandsma, T. 1996. Comparison of circulation classification schemes for predicting temperature and precipitation in the Netherlands, submitted to *Int. J. Climatol.*

Cleveland, W.S. 1979. Robust locally weighted regression and smoothing scatterplots, *J. Am. Statist. Assoc.*, **74**, 829–836.

Ceveland, W.S. and Devlin, S.J. 1988. Locally weighted regression: an approach to regression analysis by local fitting, *J. Am. Statist. Assoc.*, **83**, 596–610.

Conway, D. and Jones, P.D. 1995. The use of weather types and air flow indices for GCM downscaling, submitted to *J. Hydrol.*

Conway, D., Wilby, R.L. and Jones, P.D. 1995. Precipitation and air flow indices over the British Isles, submitted to *Clim. Res.*

Corte-Real, J., Zhang, X. and Wang, X. 1995. Downscaling GCM information to regional scales: a non-parametric multivariate regression approach, *Clim. Dyn.*, **11**, 413–424.

Gerstengarbe, F.W. and Werner, P.C. 1993. *Katalog der Grosswetterlagen Europas nach Paul Hess und Helmuth Brezowski 1881-1992*, Berichte des Deutschen Wetterdienstes nr. 113, 4th ed., Deutscher Wetterdienst, Offenbach am Main, Germany, 249 pp (in German).

Hess, P. and Brezowski, H. 1969. *Katalog der Grosswetterlagen Europas*, Berichte des Deutschen Wetterdienstes nr. 113, vol. 15, 2nd ed., Deutscher Wetterdienst, Offenbach am Main, Germany, 70 pp. (in German).

Jenkinson, A.F. and Collison, F.P. 1977. *An initial climatology of gales over the North Sea*, Synoptic Climatology Branch Memorandum no. 62, Meteorological Office, Bracknell (unpublished). Available from the National Meteorological Library, Meteorological Office, Bracknell, U.K.

Jones, P.D., Hulme, M. and Briffa, K.R. 1993. A comparison of Lamb circulation types with an objective classification scheme, *Int. J. Climatol.*, **13**, 655–663.

Kruizinga, S. 1978. *Objectieve classificatie van dagelijkse 500 mbar patronen*, Scientific report W.R. 78–8, KNMI, De Bilt, the Netherlands, 34 pp. (in Dutch).

Kruizinga, S. 1979. Objective classification of daily 500 mbar patterns, In: *preprints Sixth Conference on Probability and Statistics in Atmospheric Sciences, October 9–12, 1979, Banff, Alberta, Canada*, 126–129, AMS, Boston, Mass.

Lamb, H.H. 1972. British Isles weather types and a register of the daily sequence of circulation patterns, 1861–1971, *Geophysical Memoir*, **116**, HMSO, London, 85 pp.

Lemcke, C. and Kruizinga, S. 1988. Model output statistics forecasts: three years of operational experience in the Netherlands, *Mon. Wea. Rev.*, **116**, 1077–1090.

Wilby, R.L., Barnsley, N. and O'Hare, G. 1995. Rainfall variability associated with Lamb weather types: the case for incorporating weather fronts, *Int. J. Climatol.*, **15**, 1241–1252.